Patients With Acute-on-Chronic Liver Failure Have Increased Numbers of Regulatory Immune Cells Expressing the Receptor Tyrosine Kinase MERTK

Bernsmeier, Christine; Pop, Oltin T; Singanayagam, Arjuna; Triantafyllou, Evangelos; Patel, Vishal C; Weston, Christopher J; Curbishley, Stuart; Sadiq, Fouzia; Vergis, Nikhil; Khamri, Wafa; Bernal, William; Auzinger, Georg; Heneghan, Michael; Ma, Yun; Jassem, Wayel; Heaton, Nigel D; Adams, David H; Quaglia, Alberto; Thursz, Mark R; Wendon, Julia

DOI:
10.1053/j.gastro.2014.11.045

Accepted Manuscript

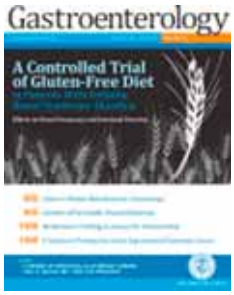

Patients with Acute on Chronic Liver Failure Have Increased Numbers of Regulatory Immune Cells Expressing the Receptor Tyrosine Kinase MERTK

Christine Bernsmeier , Oltin T. Pop , Arjuna Singanayagam , Evangelos Triantafyllou , Vishal C. Patel , Christopher J. Weston , Stuart Curbishley , Fouzia Sadiq , Nikhil Vergis , Wafa Khamri , William Bernal , Georg Auzinger , Michael Heneghan , Yun Ma , Wayel Jassem , Nigel D. Heaton , David H. Adams , Alberto Quaglia , Mark R. Thursz , Julia Wendon , Charalambos G. Antoniades

PII: S0016-5085(14)01482-6
DOI: 10.1053/j.gastro.2014.11.045
Reference: YGAST 59488

To appear in: *Gastroenterology*
Accepted Date: 26 November 2014

Please cite this article as: Bernsmeier C, Pop OT, Singanayagam A, Triantafyllou E, Patel VC, Weston CJ, Curbishley S, Sadiq F, Vergis N, Khamri W, Bernal W, Auzinger G, Heneghan M, Ma Y, Jassem W, Heaton ND, Adams DH, Quaglia A, Thursz MR, Wendon J, Antoniades CG, Patients with Acute on Chronic Liver Failure Have Increased Numbers of Regulatory Immune Cells Expressing the Receptor Tyrosine Kinase MERTK, *Gastroenterology* (2015), doi: 10.1053/j.gastro.2014.11.045.

Patients with Acute on Chronic Liver Failure Have Increased Numbers of Regulatory Immune Cells Expressing the Receptor Tyrosine Kinase MERTK

Short title: MERTK+ monocytes induce immuneparesis in ACLF

Christine Bernsmeier[1], Oltin T Pop[1], Arjuna Singanayagam[1], Evangelos Triantafyllou[1,2], Vishal C Patel[1], Christopher J Weston[2], Stuart Curbishley[2], Fouzia Sadiq[3], Nikhil Vergis[3], Wafa Khamri[3], William Bernal[1], Georg Auzinger[1], Michael Heneghan[1], Yun Ma[1], Wayel Jassem[1], Nigel D Heaton[1], David H Adams[2], Alberto Quaglia[1], Mark R Thursz[3], Julia Wendon[1], Charalambos G Antoniades[1,2,3]

[1]Institute of Liver Studies, King's College Hospital, King's College London, UK

[2]Centre for Liver Research and NIHR Biomedical Research Unit, University of Birmingham, UK

[3]Section of Hepatology, St. Mary's Hospital, Imperial College London, London, UK

Grant support: Medical Research Council (MRC)

European Association for the Study of the Liver (EASL)

Rosetrees Charitable Trust

Abbreviations:

ACLF, acute on chronic liver failure; AD, acute decompensation with no cirrhosis; APACHE II, Acute Physiology and Chronic Health Evaluation II; CCR, chemokine receptors; CD, cluster of differentiation; CLD, chronic liver disease; CLIF,

Consortium on Chronic Liver Failure; CRP, C-reactive protein; FSC, forward scatter, HLA-DR, human leucocytes antigen DR; HPF, high power filed; HUVEC, human umbilical vein endothelial cells; IL-6, interleukin-6; INR, international normalized ratio; KO, knock out; LPS, lipopolysaccharide; MELD, model of end-stage liver disease; MERTK, MER receptor tyrosine kinase; NACSELD, North American Consortium for Study of End-stage Liver Disease; NFκB, nuclear factor κB; OF, organ failure; OLT orthotopic liver transplantation; PBMC, peripheral blood mononuclear cells; pMφ, peritoneal macrophages; SIRS, systemic inflammatory response syndrome; SAPS II, Simplified Acute Physiology Score II; SOCS, suppressors of cytokine signalling; SOFA, Sequential Organ Failure Assessment score; SSC, side scatter; STAT, signal transducer and activator of transcription, TAM, tyro-3, Axl and MER; TGF-β, transforming growth factor beta; TLR, toll-like receptor; TNF-α, tumor necrosis factor alpha; WBC, white blood cells;

Correspondence:

Dr. Charalambos G Antoniades

Section of Hepatology, St Mary's Hospital, Imperial College London

10th Floor, QEQM Building, South Wharf Road

London W2 1NY, UK

E-mail: c.antoniades@imperial.ac.uk

Tel: +44 207 3312 6454; fax: +4420 7724 9369

Disclosures:

The authors disclose no conflicts.

Author contributions:

study concept and design: CB, DHA, AQ, MRT, JW, CGA

acquisition, analysis and interpretation of data: CB, NV, OTP, AS, ET, VCP, CJW, SC, FS, NV, WK, WB, GA, MH, WJ, NDH, YM, DHA, AQ, MRT, JW, CGA

drafting of the manuscript: CB, CGA

critical revision of the manuscript for important intellectual content: CB, DHA, AQ, MRT, JW, CGA

obtained funding: CGA

Abstract

Background & Aims

Characteristics of decompensated cirrhosis and acute-on-chronic liver failure (ACLF) include susceptibility to infection, immune paresis, and monocyte dysfunction. MERTK, a receptor tyrosine kinase, is expressed by monocytes and macrophages and contributes to downregulation of innate immune responses. We investigated whether MERTK expression is altered on monocytes from patients with liver failure.

Methods

We analyzed blood and liver samples collected from patients admitted to the liver intensive therapy unit at King's College Hospital, London, from December 2012 through July 2014. Patients had either ACLF (n=41), acute decompensation of cirrhosis without ACLF (n=9), cirrhosis without decompensation (n=17), or acute liver failure (n=23). We also analyzed samples from healthy individuals (controls, n=29). We used flow cytometry to determine level of innate immune function, and associated the findings with disease severity. We developed an assay to measure recruitment and migration of immune cells from the tissue parenchyma. Immunohistochemistry and confocal microscopy were used to determine levels of MERTK in bone marrow, liver, and lymph node tissues. We performed immunophenotype analyses and measured production of tumor necrosis factor and interleukin-6 and intracellular killing of *Escherichia coli* by monocytes and peritoneal macrophages incubated with lipopolysaccharide, with or without an inhibitor of MERTK (UNC569).

Results

Numbers of monocytes and macrophages that expressed MERTK were greatly increased the circulation, livers, and lymph nodes of patients with ACLF, compared to patients with stable cirrhosis and controls; MERTK expression (mean fluorescence intensity) correlated with severity of hepatic and extrahepatic disease and systemic inflammatory responses. Based on immunophenotype, migration, and functional analyses, MERTK-expressing monocytes migrate across the endothelia to localize into tissue sites and regional lymph nodes. Expression of MERTK reduced the response of cultured monocytes to lipopolysaccharide; addition of UNC569 restored production of inflammatory cytokines in response to lipopolysaccharide.

Conclusions

Patients with ACLF have increased numbers of immunoregulatory monocytes and macrophages that express MERTK and suppress the innate immune responses to microbes. Numbers of these cells correlate with disease severity and the inflammatory response. MERTK inhibitors restore production of inflammatory cytokines by immune cells from patients with ACLF, and might be developed to increase the innate immune response in these patients.

Keywords

ALF; SIRS; immune regulation; bacterial infection;

Introduction

Patients with cirrhosis exhibit a marked susceptibility to infections, developing in 35% of hospitalised patients compared to 5-7% of the general population[1]. Furthermore, infection accounts for over 50% of admissions of cirrhotic patients to hospital and is the main precipitant for the rapid decompensation referred to as 'acute-on-chronic' liver failure (ACLF), which is associated with the development of multiple organ failure. Once established, ACLF carries a prohibitively high mortality rate and a significant burden on critical care services and healthcare resources[2,3]. Impaired peripheral immune responses to microbial challenges, termed immuneparesis, is postulated to be responsible for the development of secondary infections, and is an independent predictor of mortality in ACLF[3]. Despite advances in organ failure support, there are no targeted strategies to combat susceptibility to infection in patients with cirrhosis and ACLF.

Monocyte dysfunction in ACLF, characterised by low HLA-DR and attenuated pro-inflammatory responses to microbial challenge, is associated with an adverse outcome and may account for the predisposition to infectious complications[4,5]. These observations in ACLF echo our recent findings of monocyte dysfunction and immuneparesis in acute liver failure (ALF)[6].

The MER receptor tyrosine kinase (MERTK) is a transmembrane protein of the TAM receptor family expressed on monocytes/macrophages and dendritic cells as well as epithelial cells and reproductive and neuronal tissues[7,8]. MERTK is activated by its

ligands Gas-6, Protein-S and Galectin-3, leading to receptor auto-phosphorylation and activation of the downstream signalling cascade[8].

MERTK is an important negative regulator of innate immune responses and plays a central role in resolution of inflammation through inhibition of pro-inflammatory responses to microbial challenge and promoting the clearance of apoptotic cells[8,9]. MERTK plays a pivotal role in regulation of monocyte inflammatory responses where its activation was shown to inhibit toll-like receptor (TLR) activation and cytokine-receptor induced pro-inflammatory cytokine production through downstream activation of SOCS1/3[10]. MERTK KO mice were hypersensitive to LPS and developed fatal TNF-α induced severe septic shock[11]. Moreover, elevated monocyte MERTK and Gas-6 levels have recently been reported in patients with septic shock with persistent expression associated with an adverse outcome[12,13].

In view of the recently described role of MERTK in suppressing innate immune responses, we sought to determine whether activation of this immune-regulatory pathway could account for monocyte/macrophage dysfunction, and establish its candidacy as an immunotherapeutic target to reduce susceptibility to infectious complications in patients with ACLF.

Methods

Patients and sampling

The study was approved by the King's College Hospital Ethics Committee (12/LO/0167). Assent was obtained by the patients' nominated next of kin if they were unable to give informed consent themselves. Between December 2012 and July 2014, 119 subjects were recruited to the study within 24 hours following admission to Liver Intensive Therapy Unit (LITU) or liver wards. Patients were categorised into different groups: ACLF (n=41), acute decompensation of cirrhosis with "no ACLF" (AD; n=9; according to the CLIF-SOFA classification previously described[2]), patients with cirrhosis with no evidence for acute decompensation (n=17), patients with acute liver failure (ALF; n=23) and healthy controls (HC; n=29). Cirrhosis was diagnosed by previous liver biopsy or clinical presentation with typical ultrasound or CT imaging. Exclusion criteria were: age <18 years, malignancy, immunosuppressive therapy other than corticosteroids, which were accepted if required for the treatment of autoimmune liver disease, alcoholic hepatitis or suspected relative adrenal insufficiency.

Clinical, haematological, and biochemical parameters

Full blood count, International normalized ratio (INR), liver and renal function tests, lactate, ammonia and clinical variables were prospectively entered into a database. The following disease severity scores were calculated: Child-Pugh, model of end-stage liver disease (MELD), CLIF-SOFA[2], North American Consortium for Study of End-stage Liver Disease (NACSELD)[14], Acute Physiology and Chronic Health Evaluation II (APACHE II), Simplified Acute Physiology Score II (SAPS II),

Sequential Organ Failure Assessment (SOFA) scores and infections were documented.

Isolation of monocytes

Monocytes were isolated using CD14-microbeads as described[6] or sequential depletion using CD66abce-, CD56-microbeads and Pan-Monocyte Isolation Kit (Miltenyi Biotec, Germany). Purity of monocytes was assessed by flow-cytometry (Supplementary Material and Methods).

Phenotyping of monocytes/macrophages and measurement of cytokine responses to lipopolysaccharide (LPS)

Monoclonal antibodies against CD14, CD16, CD86, CD163, CD64, CCR2, CCR5, CCR7 (BD Biosciences, UK); HLA-DR, CD32, CX3CR1 (eBioscience, UK), hMer (R&D Systems, UK) were used to determine expression of phenotypic markers on monocytes from PBMC using flow-cytometry. Results expressed as % and/or mean fluorescence intensity (MFI). TNF-α and IL-6 levels following 4-6 hour incubation of PBMC or isolated monocytes with LPS were determined by flow-cytometry based intracellular staining as previously described[6]. Flow-cytometry data was analysed using Flowlogic software, Inivai Technologies, Australia.

MERTK ligands and cytokines

Gas-6 (Abnova, Taiwan), Protein-S (Abcam, UK) were measured in plasma- and Galectin-3 (eBioscience, UK) in serum-samples using ELISA. Plasma cytokines were measured using Meso Scale Discovery (MSD; Gaithersburg, USA) as previously

described[6]. TNF-α and IL-6 in cell culture supernatants were measured as previously described[6].

Immunohistochemistry and confocal microscopy

Explanted liver tissue was obtained from patients undergoing orthotopic liver transplantation (OLT) for cirrhosis (n=6) or ACLF (n=6). Hepatic resection margins of colorectal malignancies (n=4) served as controls. Lymph nodes were obtained from 5 patients undergoing OLT for decompensated cirrhosis and 5 controls (benign stricture of left hepatic duct [n=2]; giant hepatic cyst [n=1]). Exemplarily, one bone marrow trephine from an ACLF patient was included. Tissues were taken for diagnostic histological examination, formalin-fixed and paraffin-embedded. Immunohistochemistry/multispectral imaging[6] and confocal microscopy were used to identify MERTK+CD68+, MERTK+CD163+, MERTK+Ki67+ cells (Supplementary materials and methods).

Migration assay

Human umbilical vein endothelial cells (HUVECs) were grown on collagen plugs in cell culture inserts and stimulated with TNF-α and IFN-γ. Isolated monocytes were added on top of the HUVEC/collagen matrix. After 1.5h of incubation, non-migrated monocytes were harvested. Following 24h, reverse migrated monocytes were harvested by aspiration and subendothelial monocytes were recovered from the HUVEC/collagen matrix by incubation with collagenase. Monocyte populations were analysed using a CyAn flow-cytometer (Beckman Coulter, UK) (Supplementary material and methods).

In-vitro Inhibition of MERTK signalling pathway

A small-molecule inhibitor of MERTK, UNC569[15] (Calbiochem/Millipore, UK), was used. Isolated monocytes were pre-treated with UNC569 2μM. HLA-DR expression, TNF-α/IL-6 production were assessed by flow-cytometry. Apoptotic cells were stained by Annexin-V (BD Biosciences, UK) (Supplementary material and methods).

Western Blot for p-Y-MERTK

Isolated monocytes were starved for 4h and stimulated with 20nM Gas-6 (R&D systems, UK) for 10 min. Cells were harvested and lysed in RIPA buffer (Pierce, USA) containing phosphatase- and proteinase inhibitors. Proteins were separated on 4-12% Bis-Tris NuPAGE gels (LifeTechnologies, UK) and transferred to PVDF membranes. Antibodies were obtained from Abcam, UK. (Supplementary material and methods).

Statistical analysis

Data are expressed as the median/interquartile range (IQR) unless otherwise specified. For data that did not follow a normal distribution, the significance of differences was tested using Mann-Whitney or Wilcoxon tests, Spearman's correlation coefficients were calculated. Graphs were drawn using Prism 6.0c, GraphPad, USA.

Results

Patient characteristics

Compared to compensated cirrhotic patients, patients with ACLF showed significantly higher hepatic and extrahepatic composite organ failure scores (Child-Pugh, MELD, CLIF-SOFA and NACSELD) and indices of systemic inflammatory responses: circulating white blood counts (WBC), monocytes, C-reactive protein (CRP) and SIRS score. As shown in Table S1, patients with acute decompensation and no ACLF (AD) had significantly lower disease severity scores (MELD, CLIF-SOFA, NACSELD) compared to ACLF patients. Age did not differ between groups.

The level of MER receptor tyrosine kinase (MERTK) expression on monocytes indicates disease severity, impaired anti-microbial responses and is associated with increased frequency of secondary infections in ACLF

As the MERTK signalling cascade is known to suppress pro-inflammatory responses to microbial challenge, we investigated MERTK expression on monocytes in ACLF. Whilst monocyte progenitors in the bone marrow were MERTK-negative (Figure S1B), MERTK-expressing circulating monocytes (MERTK+) were expanded in ACLF (n=34) compared to compensated cirrhotic patients (n=17) and HC (n=14) (median 35.7% vs. 5.4/8.2%, both $p<0.0001$). Importantly, MERTK+ monocytes were also markedly expanded in ALF patients (n=23), a hepatic inflammatory pathology characterised by activation of SIRS responses and immuneparesis (Figure 1A-B). Elevated MERTK expression was detected on both CD16-negative (CD14+CD16-) and CD16-positive (CD14+CD16+) monocyte subsets with highest levels on

CD14+CD16+ cells (Figure S2). Expression of MERTK was independent of the underlying aetiology of chronic liver disease (CLD) (Figure S3A).

Given the association between MERTK, disease severity and mortality in septic shock, we sought to determine whether MERTK expression on circulating monocytes could represent a biomarker of disease severity in ACLF. MERTK expression strongly correlated with the severity of hepatic and extra-hepatic disease severity-(Child-Pugh, MELD, CLIF-SOFA, NACSELD) and SIRS score (Figure 1C). Activation of SIRS responses, in the presence or absence of infection, was strongly associated with elevations in MERTK expression (Figure S4).

In order to examine the relationship between MERTK expression and responses to microbial challenge, we determined the levels of MERTK, LPS-induced pro-inflammatory cytokine secretion and intracellular killing of *E.coli* concomitantly in circulating monocytes. Compared to HC (n=10) and patients with stable cirrhosis (n=13), patients with AD (n=5) and ACLF (n=15) had significantly elevated expression of MERTK and attenuated levels of TNF-α and IL-6 following ex-vivo LPS challenge (Figure 1D-E). Moreover, LPS induced TNF-α and IL-6 production was negatively correlated to MERTK expression, MELD (Figure 1D), Child-Pugh (TNF-α:r=-0.665/p<0.0001; IL-6:r=-0.559/p=0.002), CLIF-SOFA (TNF-α:r=-0.557/p=0.003; IL-6:r=-0.543/p=0.003), NACSELD (TNF-α:r=-0.564/p=0.002; IL-6:-0.459/p=0.016) and SIRS scores (TNF-α:r=-0.548/p=0.004; IL-6:r=-0.411/p=0.037). Oxidative burst responses to *E.coli* were preserved with no significant association with outcome (Figure S5).

In ACLF patients, culture-positive infectious complications occurred at a considerably higher frequency within the first 14 days following admission to LITU (34.1%) compared to AD patients without organ failure (11.1%; Table S1). Concomitantly ACLF patients had significantly higher monocyte MERTK-expression following admission to LITU when compared to AD and stable cirrhotic patients (ACLF 35.7% vs. AD 14.36% vs. cirrhosis 5.4%, p=0.0020/p<0.0001) (Figure 1E).

We determined the temporal evolution of MERTK expression in patients with ACLF and its relationship to outcome. Overall, peak MERTK expression was detected on admission to LITU and subsequently decreased at day 3-5 following admission (n=21). When stratified according to survival, patients surviving the episode of ACLF had a significant reduction in MERTK expression whilst non-survivors did not (Figure 1F).

Phenotypic characterisation of MERTK-positive monocytes in ACLF

In order to fully characterise circulating monocytes with impaired microbial responses in ACLF, we performed detailed immunophenotypic analyses examining the levels of activation (HLA-DR, CD86), Fcγ-receptors (CD16, CD64, CD32), scavenger (CD163) and tissue-and lymph node homing markers (CCR2, CCR5, CX3CR1, CCR7) in the whole monocyte population. Circulating monocytes in ACLF (n=9) exhibited an anti-inflammatory phenotype ($CD163^{high}HLA\text{-}DR_{low}CD86_{low}$) with significant higher expression of tissue- and lymph node homing receptors ($CCR5^{high}CCR7^{high}$) and Fcγ-receptors ($CD32^{high}CD64^{high}$) when compared to HC (n=9) (Figures 2A,S5).

Having established the relationship between the magnitude of MERTK expression and impaired microbial responses, we sought to further define the MERTK+ subpopulation of circulating monocytes expanded in patients with ACLF (Figure 2B-C). Phenotypic analysis of the MERTK+ monocyte subpopulation (MERTK+; 36% [Figure 1A]) displayed significantly higher expression of CD16, HLA-DR, CD86, CD163 and CCR7 compared to MERTK-negative cells consistent with the phenotype of a more mature and differentiated monocyte lineage (Figure 2D).

Elevated circulating ligands and constitutive receptor phosphorylation indicate activation of the MERTK signalling cascade in ACLF

To identify ligands that activate the MERTK signalling pathway in ACLF, we measured circulatory levels of Gas-6, Galectin-3 and Protein-S. The plasma concentrations of all measured MERTK ligands were elevated in stable cirrhotic patients compared to HC. Moreover, Gas-6 and Galectin-3 were significantly higher in ACLF compared to HC (Figure 3A-C). Gas-6 and Galectin-3 levels did not correlate with MERTK-expression on monocytes and were independent of the underlying aetiology of CLD (Figure S3B-C).

Ligand-induced receptor-auto-phosphorylation activates the MERTK cascade. To investigate whether higher surface expression of MERTK in ACLF reflects its activation, tyrosine-phosphorylation of MERTK upon Gas-6 stimulation was investigated on isolated monocytes ex-vivo. In comparison to healthy monocytes, which were phosphorylated in response to Gas-6, constitutive phosphorylation and unresponsiveness to Gas-6 stimulation was detected on monocytes from a

representative patient with ACLF indicating constitutive activation of the MERTK cascade (Figure 3D).

Systemic microenvironmental factors in ACLF plasma induce a distinct MERTK-positive monocyte phenotype

As MERTK expression correlated with SIRS responses (Figures 1C,S4A-E), circulating inflammatory cytokines are likely to induce an expansion of MERTK+ monocytes in ACLF. Monocyte MERTK expression is modulated through activation of cytokine receptors by their ligands[8] (e.g. IL-10[16]). In line with previous data[4], we detect a distinct cytokine profile in patients with ACLF revealing high levels of TNF-α, IL-6, IL-10 and IL-8 in comparison to HC and cirrhotic patients respectively (Figure S6). Monocyte MERTK expression positively correlated with plasma levels of TNF-α, IL-6, IL-8 and IL-10 (Figure 3E). Corticosteroid-treated ACLF patients were characterised by significantly higher disease severity scores (MELD, CLIF-SOFA, both $p<0.0001$) and MERTK expression (Figure S4F).

To assess the influence of the systemic inflammatory microenvironment on monocyte function in ACLF, we studied phenotype and function of healthy monocytes after conditioning in plasma derived from ACLF patients and healthy donors. Culture in the presence of ACLF plasma induced a distinct phenotype ($MERTK^{high}CD163^{high}HLA\text{-}DR_{low}CCR7^{high}$) resembling that described for monocytes ex-vivo with attenuated pro-inflammatory responses but higher oxidative burst responses to *E.coli* (Figures S5,S7-8).

MERTK-positive monocytes have reinforced potential to migrate across endothelial layers

Following an infectious insult, circulating monocytes migrate across the endothelium into tissues where they differentiate into macrophages and promote anti-microbial responses[17]. Subsequently, they home to regional lymph nodes to elicit immune responses, or may return to the circulatory pool. We examined migratory characteristics of monocytes from ACLF patients across the endothelium into the subendothelial space and back across the endothelium (reverse-migration) using a novel in-vitro migration model. Reverse migration recapitulates the in-vivo pathway through which tissue monocytes/macrophages home to regional lymph nodes or re-join the circulatory pool[18].

A significantly higher percentage and number of MERTK+ monocytes underwent transendothelial migration and reverse migration when compared to HC (Figure 4A-C). Cells that did not migrate were more often MERTK-. Analyses of reverse-migrated monocytes revealed a $MERTK^{high}CD163^{high}$ phenotype (Figure 4C) similar to the MERTK+ subpopulation described in ACLF monocytes ex-vivo (Figure 2D). The in-vitro data imply that MERTK+ monocytes exhibit a preferential migratory pattern across endothelia, home into extracirculatory compartments and suppress tissue-specific immune responses.

Endothelial dysfunction in cirrhosis[19] may also promote the migration of monocytes/macrophages into tissues. We detect elevated levels of systemic- (sICAM-1 and sVCAM-1) and tissue (angiopoietin-2) specific-markers of endothelial dysfunction and leakage in patients with cirrhosis and ACLF (Figure S9).

ACLF is characterised by an expansion of immunoregulatory, MERTK-positive macrophages in tissue compartments and regional lymph nodes

In view of our data revealing an expansion of MERTK+ monocytes in the circulation of patients with ACLF, that preferentially migrate across the endothelium, we examined these cells in the peritoneal cavity, livers and regional lymph nodes.

The percentage of MERTK-expressing peritoneal macrophages (pMφ) was significantly higher when compared to their circulatory counterparts (67.5% vs. 24.8%, p=0.0079) (Figure 4D). The pMφ phenotype was characterised by elevated expression of pro-resolution/anti-inflammatory and tissue- and lymph node homing markers: HLA-DR^{high}CD163^{high}CX3CR1^{high}CCR7^{high} (Figure S10). Analysis of MERTK+ pMφ subset shows a HLA-DR^{high}CD163^{high}CCR7^{high} phenotype that bears striking phenotypic and functional similarities to their circulatory counterparts described above (Figure 4E-F).

Using multispectral analysis and confocal microscopy of liver explant tissue, we show a significant expansion of MERTK^{high}CD163^{high} hepatic macrophages in ACLF patients when compared to cirrhotic patients without organ failure who underwent transplantation (n=6 each) and to pathological control tissue (n=4) (Figure 5A-B; Figure S1). MERTK+ macrophages were predominantly Ki-67 negative, suggesting they are recruited rather than resident in origin.

Having documented a high expression of lymph node (LN) homing receptor, CCR7, on circulating monocytes and pMφ, and, in view of the importance of LN

macrophages in filtering of tissue-derived pathogens and triggering anti-microbial responses, we evaluated MERTK expression in mesenteric lymph nodes (MLN) from patients with decompensated cirrhosis (n=5) and pathological controls (n=3). MERTK+/CD68+ MLN macrophages were markedly increased in decompensated cirrhotic patients compared to controls (185 vs. 90 cells/10HPF;p=0.0357). Strikingly, MERTK+ macrophages were distributed in both subcapsular and medullary (termed extra-follicular) regions of the LN (111 vs. 21 cells/10HPF;p=0.0357) (Figures 5C-D, S1), suggesting they enter both through lymphatics and high endothelial venules into areas where macrophages play a crucial role in triggering innate and adaptive anti-microbial responses[20].

Inhibition of MERTK restores pro-inflammatory responses in ACLF

As MERTK+ monocytes exhibited attenuated response to LPS challenge, inhibition of the MERTK signalling pathway may restore monocyte responses to microbial challenge. In a series of in-vitro experiments, ACLF (MERTK+ 69.9%) and HC-conditioned monocytes (MERTK+ 51.6%) were cultured in the presence and absence of MERTK-inhibitor UNC569 (Figure 6A). Culture of monocytes with UNC569 (2μM) for 24h significantly up-regulated activation marker HLA-DR in ACLF (n=10) but not HC (n=6) (Figure 6B). In ACLF, UNC569 (2 μM) treatment for 6h led to a significant increase in both LPS-induced TNF-α and IL-6 production but not intracellular killing of *E.coli* (Figures 6C-D,S5; n=4 each). There was no increase in apoptotic cells in the UNC569 treated ACLF monocytes in-vitro (1.3 vs. 1.2%, p=0.968).

Discussion

The marked expansion of an immunoregulatory, MERTK-expressing monocyte/macrophage population is a novel finding in the pathogenesis of immuneparesis in ACLF. In particular, the magnitude of MERTK expression on circulating monocytes strongly correlated with suppression of innate immune responses to microbial challenge, suggesting that MERTK may serve as a marker of innate immune dysfunction in ACLF. Further analyses reveal that these monocytes express the anti-inflammatory ($CD163^{high}HLA\text{-}DR_{low}$) phenotype that has been extensively described in other hepatic[4-6] and systemic inflammatory pathologies[21] where there is immuneparesis and susceptibility to infectious complications.

The biological relevance of this immunoregulatory, MERTK+ monocyte phenotype in ACLF is highlighted through its strong relationship with hepatic and extrahepatic disease severity scores (Child-Pugh, MELD, CLIF-SOFA, NACSELD) and with the magnitude of SIRS response, irrespective of the presence or absence of infection. This significant finding corroborates previous reports identifying the importance of SIRS during the evolution of ACLF[4].

Immune profiling of circulating monocytes in ACLF reveals that the major defect in innate responses is the impairment of pro-inflammatory responses to microbial challenge. These findings are corroborated by a number of previous publications by us and others[4,5,22]. However, we did not detect defects in ex-vivo bacterial killing, as recently reported in patients with decompensated cirrhosis (AD)[23]. These findings are perhaps not surprising in view of the fact that monocytes exhibit marked

functional plasticity during a given inflammatory insult. Our findings could be explained by the fact that activation of SIRS responses, that define the transition from AD to ACLF, enhance the production of reactive oxygen species and the bacterial killing ability of monocytes[24]. Further studies are needed to dissect defects in innate immune dysfunction during the clinical evolution of disease.

We moreover identified a higher frequency of infectious complications in those patients who had higher MERTK expression and severity of organ failure. To our knowledge, this is the first description of a biomarker linking and possibly predicting disease severity and immuneparesis. Large prospective studies are warranted to assess its utility in patients with ACLF.

Our data reveal a marked expansion of MERTK+ monocytes/macrophages in tissue compartments (e.g. peritoneum, liver) and in mesenteric lymph nodes, where monocytes/macrophages are recruited via afferent lymphatics draining regional tissue compartments. Characterisation of peritoneal MERTK+ macrophages reveals striking phenotypic (HLA-DR^{high}CD163^{high}) and functional (attenuated pro-inflammatory responses) similarities with their circulatory counterparts. Analyses of ACLF liver tissue also show a macrophage rich infiltrate bearing a MERTK^{high}CD163^{high} phenotype particularly within the hepatic sinusoids. These data suggest that MERTK+ monocytes/macrophages accumulate in different tissue compartments in ACLF.

We reveal that a high proportion of MERTK-bearing monocytes and peritoneal macrophages express tissue and lymph node homing receptors. Moreover, we show

that these monocytes have enhanced migratory capabilities, and are able to migrate efficiently across endothelia from blood to tissue and then out of tissue bearing the characteristic MERTK^{high}CD163^{high} phenotype. Apart from the enhanced migratory capabilities of MERTK+ monocytes, endothelial dysfunction in CLD[19] and organ failure[25] might further facilitate their tissue homing capabilities. In line with this theory, angiopoietin-2, a marker of endothelial "leakage" in cirrhosis[19] was highly expressed in hepatic endothelia in cirrhosis and ACLF patients.

The data suggest that a dynamic circulatory pathway exists where MERTK+ cells traffick from tissue sites to regional lymph nodes and back to the circulation. In support of this theory, we observed a striking increase in the number of subcapsular sinus and medullary cord (extra follicular) macrophages expressing MERTK in the mesenteric lymph nodes from patients with decompensated cirrhosis. The low number of resident, proliferating monocytes/macrophages support that they are predominantly recruited from the circulatory monocyte pool. These macrophages serve to "filter" tissue and lymph borne pathogens, preventing their systemic translocation and priming innate and adaptive immune responses[26]. Taken together, we hypothesise that the increase in MERTK+ macrophages in mesenteric lymph nodes is of major pathogenic significance contributing to suppression of innate immune responses to microbial challenge in patients with ACLF.

The strong correlation of MERTK expression with SIRS and circulatory cytokines on the one hand and with liver disease severity on the other hand, supports the notion that both systemic and intrahepatic inflammatory events in ACLF mould monocytes towards a MERTK+ phenotype. Our data demonstrate that monocytes acquire

MERTK expression once they exit the bone marrow and are exposed to circulating inflammatory mediators in ACLF plasma. Circulatory inflammatory factors favouring monocyte differentiation towards a MERTK+ phenotype include MERTK ligands, cytokines and corticosteroids[27]. We observed elevated levels of MERTK ligands (Gas-6, galectin-3) and inflammatory cytokines in patients with cirrhosis and ACLF, suggesting these mediators may modulate monocyte MERTK expression. The positive correlation of MERTK expression with TNF-α, IL-6 and IL-10 might indicate a role for these cytokines in inducing MERTK in ACLF. Cytokines have been reported to induce TAM receptor activation[10], in particular IL-10 has previously been shown to up-regulate MERTK expression[16]. ACLF patients treated with corticosteroids had significantly higher disease severity scores and MERTK expression. The effect of inflammatory mediators and steroid treatment on MERTK expression alone cannot be distinguished in this ACLF cohort.

Data from patients with ALF revealing high disease severity, SIRS and high MERTK but low steroid treatment rate suggest that circulating inflammatory mediators (e.g. IL-10) are likely to be the main triggers for MERTK expression. However, further work is necessary to dissect how different mediators modulate MERTK expression on monocytes in ACLF.

During acute liver injury, hepatocyte death triggers an expansion of resolution macrophages in the liver[6]. The magnitude of hepatocellular apoptosis has previously been linked to disease severity in ACLF[28]. Resolution of tissue inflammation requires activation of MERTK-dependant pathways, triggered by the surface expression of phosphatidylserine on apoptotic cells[9]. Consequently, activation of MERTK-mediated uptake of apoptotic cells might contribute to the expansion of the MERTK+

macrophage population we describe in ACLF. The role of hepatocyte death as a driver of MERTK expression is corroborated by its strong correlation with liver-specific disease severity scores. Equally, apoptosis of parenchymal cells in other epithelial beds (e.g. kidney[29]) may also promote MERTK+ monocytes/macrophages during the evolution of organ failure in ACLF.

In Figure 7, we provide a mechanistic explanation to account for the expansion of MERTK+ monocyte/macrophages in the circulation and tissue compartments of patients with ACLF. Here, we propose that systemic inflammatory mediators and repeated cycles of migration in and out of inflamed tissues, facilitated by endothelial dysfunction, results in up-regulation of MERTK and suppression of innate immune responses.

Immuneparesis had previously been linked to secondary infections, which are the major cause of death in patients with ACLF[3,4]. Current treatment involves prophylactic and targeted antibiotic agents, which contribute to the emergence of antimicrobial resistance and often do not prevent recurrent infections. Strategies enhancing innate immune responses might be beneficial in preventing secondary infection and improving outcome. Having identified an immunoregulatory monocyte population, we evaluated its candidacy as a future immunotherapeutic target. MERTK negatively regulates pro-inflammatory-responses to microbial challenge[14] and therefore represents a promising target. This is supported by our experiments showing that MERTK inhibition in ACLF monocytes in-vitro leads to up-regulation of their activation marker, HLA-DR, and to enhanced response to microbial challenge and is consistent with recent reports where inhibition of MERTK restored LPS-

induced pro-inflammatory response in a STAT1-SOCS1/3-NFκB dependant manner[30]. Absence of MERTK in microenvironmental leucocytes stimulated anti-tumour immune responses in mice[31]. In humans, MERTK inhibitors are being evaluated for the treatment of cancer such as glioblastoma[32] and might be accessible in ACLF.

In view of our findings, we hypothesise that an immunotherapeutic strategy, aimed at inhibiting MERTK and restoring monocyte responses to bacterial challenge, is likely to be of clinical benefit if instituted early in disease evolution in order to prevent attendant secondary infections. The dynamic evolution of innate immune defects exemplifies the importance of immune profiling before embarking on immunostimulatory therapeutic strategies. Further studies are warranted to identify the optimal strategy aimed at boosting innate immune response in ACLF.

In conclusion, our data reveal a marked expansion of MERTK expressing, immunoregulatory monocytes/macrophages in the circulation and in tissues in patients with ACLF that strongly correlates with indices of liver disease severity and activation of SIRS responses. Functionally MERTK+ cells have attenuated response to microbial challenge, which might explain predisposition to secondary infection in ACLF. Furthermore, we have identified a mechanism that is key to monocyte/macrophage dysregulation and immuneparesis in ACLF and provides a novel immunotherapeutic target aimed at restoring innate immune responses to microbial challenge and reducing susceptibility to infections.

Acknowledgements

We gratefully acknowledge Dr. Adrian Bomford and Dr. Chris Willars for help with recruitment, Dr. Ragai Mitry for methodological support and Dr. Reinhard Bernsmeier for help with the clinical database. Moreover we gratefully acknowledge all patients and families who consented to take part in this study and all staff at King's College Hospital involved in these patients' care.

We thank the Medical Research Council (MRC), the European Association for the Study of the Liver (EASL) and Rosetrees and Stoneygate Charitable Trust for ongoing funding support and King's College Hospital Research & Development, the Imperial National Institute of Health Research Biomedical Research Centre and the Centre for Liver Research and NIHR Biomedical Research Unit, University of Birmingham for infrastructure support.

References

1. Borzio M, Salerno F, Piantoni L, et al. Bacterial infection in patients with advanced cirrhosis: a multicentre prospective study. Dig. Liver Dis. Off. J. Ital. Soc. Gastroenterol. Ital. Assoc. Study Liver 2001;33:41–48.

2. Moreau R, Jalan R, Gines P, et al. Acute-on-chronic liver failure is a distinct syndrome that develops in patients with acute decompensation of cirrhosis. Gastroenterology 2013;144:1426–1437, 1437.e1–9.

3. Bajaj JS, O'Leary JG, Reddy KR, et al. Second infections independently increase mortality in hospitalized patients with cirrhosis: the North American consortium for the study of end-stage liver disease (NACSELD) experience. Hepatol. Baltim. Md 2012;56:2328–2335.

4. Wasmuth HE, Kunz D, Yagmur E, et al. Patients with acute on chronic liver failure display "sepsis-like" immune paralysis. J. Hepatol. 2005;42:195–201.

5. Berry P, Antoniades C, Carey I, et al. Severity of the compensatory anti-inflammatory response determined by monocyte HLA-DR expression may assist outcome prediction in cirrhosis. Intensive Care Med. 2011;37:453–460.

6. **Antoniades CG, Khamri W**, Abeles RD, et al. Secretory leukocyte protease inhibitor: a pivotal mediator of anti-inflammatory responses in acetaminophen-induced acute liver failure. Hepatol. Baltim. Md 2014;59:1564–1576.

7. **Graham DK, Dawson TL**, Mullaney DL, et al. Cloning and mRNA expression analysis of a novel human protooncogene, c-mer. Cell Growth Differ. Mol. Biol. J. Am. Assoc. Cancer Res. 1994;5:647–657.

8. Lemke G, Rothlin CV. Immunobiology of the TAM receptors. Nat. Rev. Immunol. 2008;8:327–336.

9. Scott RS, McMahon EJ, Pop SM, et al. Phagocytosis and clearance of apoptotic cells is mediated by MER. Nature 2001;411:207–211.

10. Rothlin CV, Ghosh S, Zuniga EI, et al. TAM receptors are pleiotropic inhibitors of the innate immune response. Cell 2007;131:1124–1136.

11. Camenisch TD, Koller BH, Earp HS, et al. A novel receptor tyrosine kinase, Mer, inhibits TNF-alpha production and lipopolysaccharide-induced endotoxic shock. J. Immunol. Baltim. Md 1950 1999;162:3498–3503.

12. **Guignant C, Venet F**, Planel S, et al. Increased MerTK expression in circulating innate immune cells of patients with septic shock. Intensive Care Med. 2013;39:1556–1564.

13. Gibot S, Massin F, Cravoisy A, et al. Growth arrest-specific protein 6 plasma concentrations during septic shock. Crit. Care Lond. Engl. 2007;11:R8.

14. Bajaj JS, O'Leary JG, Reddy KR, et al. Survival in infection-related acute-on-chronic liver failure is defined by extrahepatic organ failures. Hepatol. Baltim. Md 2014;60:250–256.

15. Christoph S, Deryckere D, Schlegel J, et al. UNC569, a novel small-molecule mer inhibitor with efficacy against acute lymphoblastic leukemia in vitro and in vivo. Mol. Cancer Ther. 2013;12:2367–2377.

16. Jung M, Sabat R, Krätzschmar J, et al. Expression profiling of IL-10-regulated genes in human monocytes and peripheral blood mononuclear cells from psoriatic patients during IL-10 therapy. Eur. J. Immunol. 2004;34:481–493.

17. Gordon S, Taylor PR. Monocyte and macrophage heterogeneity. Nat. Rev. Immunol. 2005;5:953–964.

18. Randolph GJ, Furie MB. Mononuclear phagocytes egress from an in vitro model of the vascular wall by migrating across endothelium in the basal to apical direction: role of intercellular adhesion molecule 1 and the CD11/CD18 integrins. J. Exp. Med. 1996;183:451–462.

19. Melgar-Lesmes P, Tugues S, Ros J, et al. Vascular endothelial growth factor and angiopoietin-2 play a major role in the pathogenesis of vascular leakage in cirrhotic rats. Gut 2009;58:285–292.

20. Kuka M, Iannacone M. The role of lymph node sinus macrophages in host defense. Ann. N. Y. Acad. Sci. 2014;1319:38–46.

21. Landelle C, Lepape A, Voirin N, et al. Low monocyte human leukocyte antigen-DR is independently associated with nosocomial infections after septic shock. Intensive Care Med. 2010;36:1859–1866.

22. Antoniades CG, Wendon J, Vergani D. Paralysed monocytes in acute on chronic liver disease. J. Hepatol. 2005;42:163–165.

23. O'Brien AJ, Fullerton JN, Massey KA, et al. Immunosuppression in acutely decompensated cirrhosis is mediated by prostaglandin E2. Nat. Med. 2014;20:518–523.

24. **Martins PS, Brunialti MKC**, Martos LSW, et al. Expression of cell surface receptors and oxidative metabolism modulation in the clinical continuum of sepsis. Crit. Care Lond. Engl. 2008;12:R25.

25. David S, Kümpers P, Slyke P van, et al. Mending leaky blood vessels: the angiopoietin-Tie2 pathway in sepsis. J. Pharmacol. Exp. Ther. 2013;345:2–6.

26. **Kastenmüller W, Torabi-Parizi P**, Subramanian N, et al. A spatially-organized multicellular innate immune response in lymph nodes limits systemic pathogen spread. Cell 2012;150:1235–1248.

27. Zagórska A, Través PG, Lew ED, et al. Diversification of TAM receptor tyrosine kinase function. Nat. Immunol. 2014;15:920–928.

28. Zheng S-J, Liu S, Liu M, et al. Prognostic value of M30/M65 for outcome of hepatitis B virus-related acute-on-chronic liver failure. World J. Gastroenterol. WJG 2014;20:2403–2411.

29. Shah N, Mohamed FE, Jover-Cobos M, et al. Increased renal expression and urinary excretion of TLR4 in acute kidney injury associated with cirrhosis. Liver Int. Off. J. Int. Assoc. Study Liver 2013;33:398–409.

30. Lee Y-J, Han J-Y, Byun J, et al. Inhibiting Mer receptor tyrosine kinase suppresses STAT1, SOCS1/3, and NF-κB activation and enhances inflammatory

responses in lipopolysaccharide-induced acute lung injury. J. Leukoc. Biol. 2012;91:921–932.

31. Cook RS, Jacobsen KM, Wofford AM, et al. MerTK inhibition in tumor leukocytes decreases tumor growth and metastasis. J. Clin. Invest. 2013;123:3231–3242.

32. Knubel KH, Pernu BM, Sufit A, et al. MerTK inhibition is a novel therapeutic approach for glioblastoma multiforme. Oncotarget 2014;5:1338–1351.

Author names in bold designate shared co-first authorship.

Figure legends

Figure 1. MERTK expression and innate responses in circulatory monocytes in ACLF A. MERTK expressing monocytes (%CD14+ cells) in ACLF (n=34), ALF (n=23), cirrhosis (n=17) and healthy controls (n=14). B. Representative FACS-plot to determine MERTK expressing CD14+ monocytes. C. Correlation of MERTK expression with Child-Pugh, MELD, CLIF-SOFA, NACSELD, SIRS scores. D. LPS-induced TNF-α/IL-6-production in stable cirrhosis, AD, ACLF and correlation with MERTK expression and MELD. E. MERTK expression in cirrhosis (n=17), AD (n=7), ACLF (n=34) (%CD14+ cells). F. Sequential MERTK expression (admission; day 3-5 following admission for ACLF).

Figure 2. Phenotypic characterisation of circulating monocytes in ACLF A. Immunophenotyping of monocytes in ACLF compared to healthy controls reveals a MERTK^{high}/HLA-DR$_{low}$/CD163^{high}/CCR5^{high}/CCR7^{high} phenotype. B. Representative FACS-plot to assess the phenotype of the MERTK+ subpopulation. C. MERTK+ monocytes in ACLF (n=30), cirrhosis (n=8) and healthy controls (n=14). D. The immunophenotype of MERTK+ monocytes in ACLF is HLA-DR^{high}/CD16^{high}/CD163^{high}/CCR7^{high}.

Figure 3. Activation of the MERTK signalling cascade in ACLF. A-C. Elevation of MERTK ligands Gas-6 (pg/ml), Galectin-3 (ng/ml) and Protein-S (µg/ml) in ACLF (n=35), cirrhosis (n=11) and healthy controls (n=15). D. Immunoblotting for phospho-Y-MERTK in response to Gas-6-stimulation (20nM) on isolated monocytes from a healthy control and an ACLF patient ex-vivo. E. Correlation of plasma cytokine levels

of patients with cirrhosis and ACLF with monocyte MERTK expression (n=60). ** p<0.01.

Figure 4. MERTK+ monocytes preferentially migrate across endothelia in an in-vitro model and are expanded in the peritoneal cavity ex-vivo. A. MERTK+ monocytes conditioned in ACLF- and healthy plasma. B. Percent of migrated (subendothelial) MERTK+ monocytes in ACLF- (n=5) vs. healthy controls (n=4). C. Left: Number of non-migrated, subendothelial and reverse migrated MERTK+ and MERTK- cells/µl.; Right: %CD14+ monocytes expressing CD163, HLA-DR in different in-vitro compartments. D. Representative FACS-plot to assess phenotype of MERTK+ vs. MERTK- peritoneal macrophages (pMφ) (left) in patients with cirrhosis and ascites. %MERTK+ vs. MERTK- subpopulations in circulatory monocytes and pMφ (right). E. Immunophenotype of MERTK+ and MERTK- pMφ. F. LPS- induced TNF-α/IL-6-production in pMφ. *, p<0.05, **p<0.01.

Figure 5. MERTK expressing macrophages accumulate in the liver and in mesenteric lymph nodes in patients with ACLF and decompensated cirrhosis. A. Immunostaining for MERTK+ and MERTK+/CD163+ macrophages in pathological control, cirrhotic and ACLF liver tissue(200x), (Inset: composite pseudo-fluorescent images from multispectral analysis[400x]). Right panel: Representative confocal image of double-epitope fluorescent immunostaining for CD68(green)/MERTK(red)/co-localisation(yellow) on ACLF liver tissue confirming MERTK expression in macrophages(400x). B. Enumeration of CD163+/MERTK+ macrophages in hepatic plates of control (n=4), cirrhosis (n=6), and ACLF (n=6) liver tissue (cells/10 high power fields [HPF]). C. Immunostaining for MERTK+ and

MERTK+/CD68+ macrophages in follicular and non-follicular areas of regional lymph nodes from controls (n=3) and decompensated cirrhosis (n=5) (200×) (Insets: composite pseudo-fluorescent images from multispectral analysis[400x]). Right panels: Confocal images of double-epitope fluorescent immunostaining for CD68(green)/MERTK(red)/co-localisation(yellow) in non-follicular lymph nodes areas confirming MERTK expression in CD68+ macrophages(400×). D. Number (cells/10HPF; left and middle panels) and % of MERTK+ cells (right panel) in lymph nodes follicular and non-follicular areas.

Figure 6. **MERTK-inhibition by UNC569 improves LPS-response to microbial challenge in ACLF monocytes in-vitro.** A. Expansion of MERTK+ monocytes after conditioning of healthy monocytes in ACLF- compared to healthy plasma (%CD14+ cells). Graph shows mean+/-SEM. B. Expression of HLA-DR after UNC569(2μM) treatment in-vitro for 24h. ACLF n=10, healthy n=6. C-D. LPS-induced TNF-α and IL-6 production after UNC569(2μM) treatment for 6h.

Figure 7. Mechanistic model explaining the expansion of MERTK-positive, immunoregulatory monocytes/macrophages in ACLF as a multisystem disorder. Circulating monocytes derived from the bone marrow do not express MERTK (MERTK-; green) (1). In the circulatory microenvironment in ACLF, with high levels of IL-10, IL-6, TNF-α and Gas-6, monocytes differentiate and express MERTK (MERTK+; orange) (2). MERTK+ monocytes express tissue homing receptors and preferentially migrate across endothelia into sites of inflammation/infection (e.g. liver, peritoneum [3]). Predominantly in the liver and extrahepatic sites of inflammation, infiltrated MERTK+ monocytes interact with phosphatidylserine on apoptotic cells,

induce their clearance and further up-regulation of MERTK (4). Tissue monocytes/macrophages are phenotypically MERTK^{high}/CD163^{high}/HLA-DR^{high}, functionally endotoxin tolerant (red) and migrate to regional lymph nodes (5). MERTK+ monocytes/macrophages with enhanced migratory potential return to the circulation (reverse migration [6]). Expansion of MERTK^{high}/CD163^{high}/HLA-DR^{high}, immunoregulatory monocytes in ACLF (red) occurs in inflamed tissues, lymph nodes and the circulation.

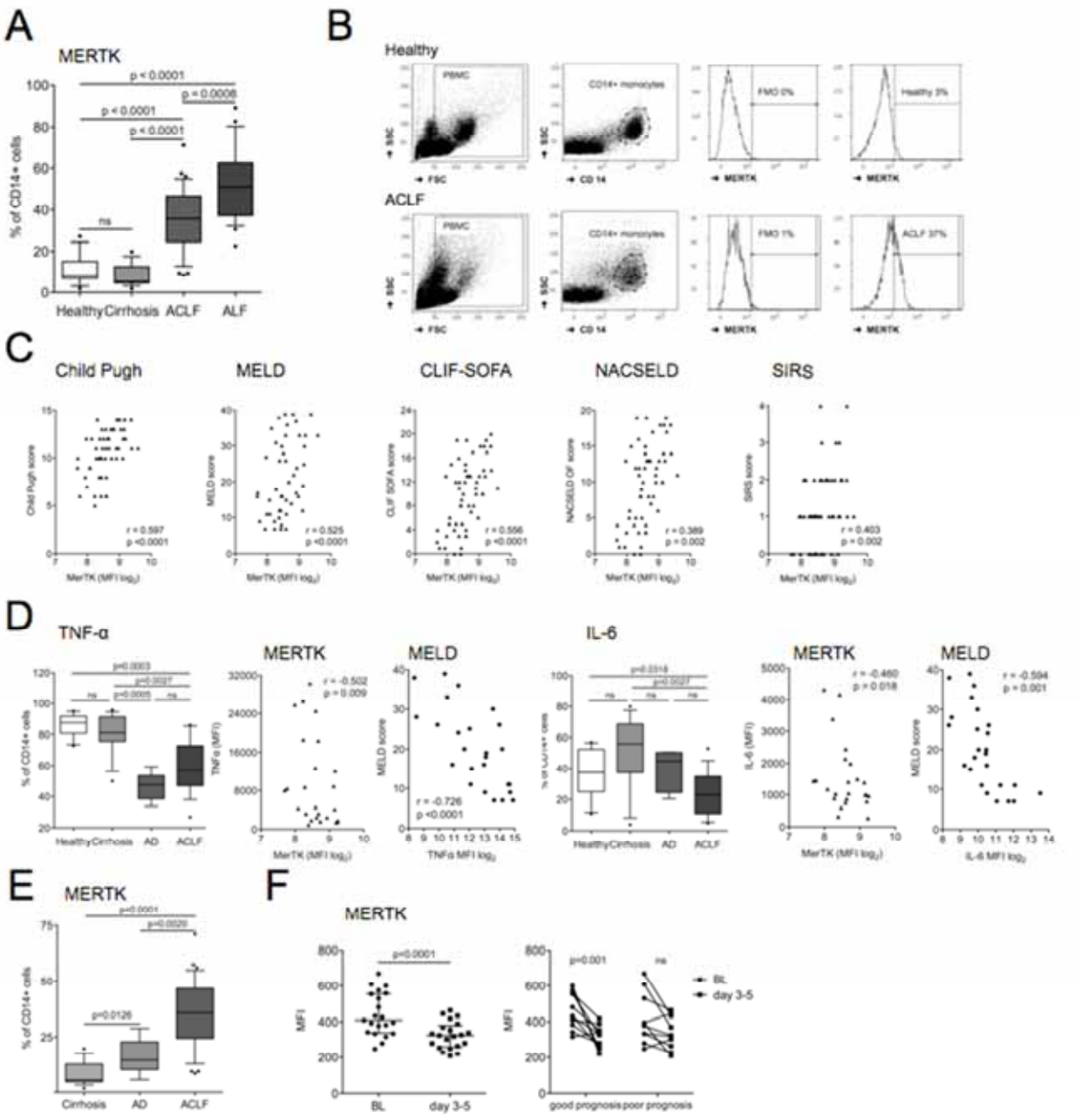
A
MERTK
% of CD14+ cells
p < 0.0001
p = 0.0006
p < 0.0001
p < 0.0001
ns
Healthy
Cirrhosis
ACLF
ALF
B
Healthy
PBMC
CD14+ monocytes
FMO 0%
Healthy 3%
FSC
SSC
CD 14
MERTK
ACLF
FMO 1%
ACLF 37%
C
Child Pugh
MELD
CLIF-SOFA
NACSELD
SIRS
Child Pugh score
MELD score
CLIF SOFA score
NACSELD OF score
SIRS score
r = 0.597
p <0.0001
r = 0.525
p <0.0001
r = 0.556
p <0.0001
r = 0.389
p = 0.002
r = 0.403
p = 0.002
MerTK (MFI log2)
D
TNF-α
IL-6
MERTK
MELD
% of CD14+ cells
TNFα (MFI)
MELD score
% of IL6+ cells
IL-6 (MFI)
r = -0.502
p = 0.009
r = -0.726
p <0.0001
r = -0.460
p = 0.018
r = -0.594
p = 0.001
HealthyCirrhosis
AD
ACLF
MerTK (MFI log2)
TNFα MFI log2
IL-6 MFI log2
E
MERTK
% of CD14+ cells
p=0.0126
Cirrhosis
AD
ACLF
F
MERTK
MFI
p=0.0001
BL
day 3-5
p=0.001
ns
good prognosis
poor prognosis

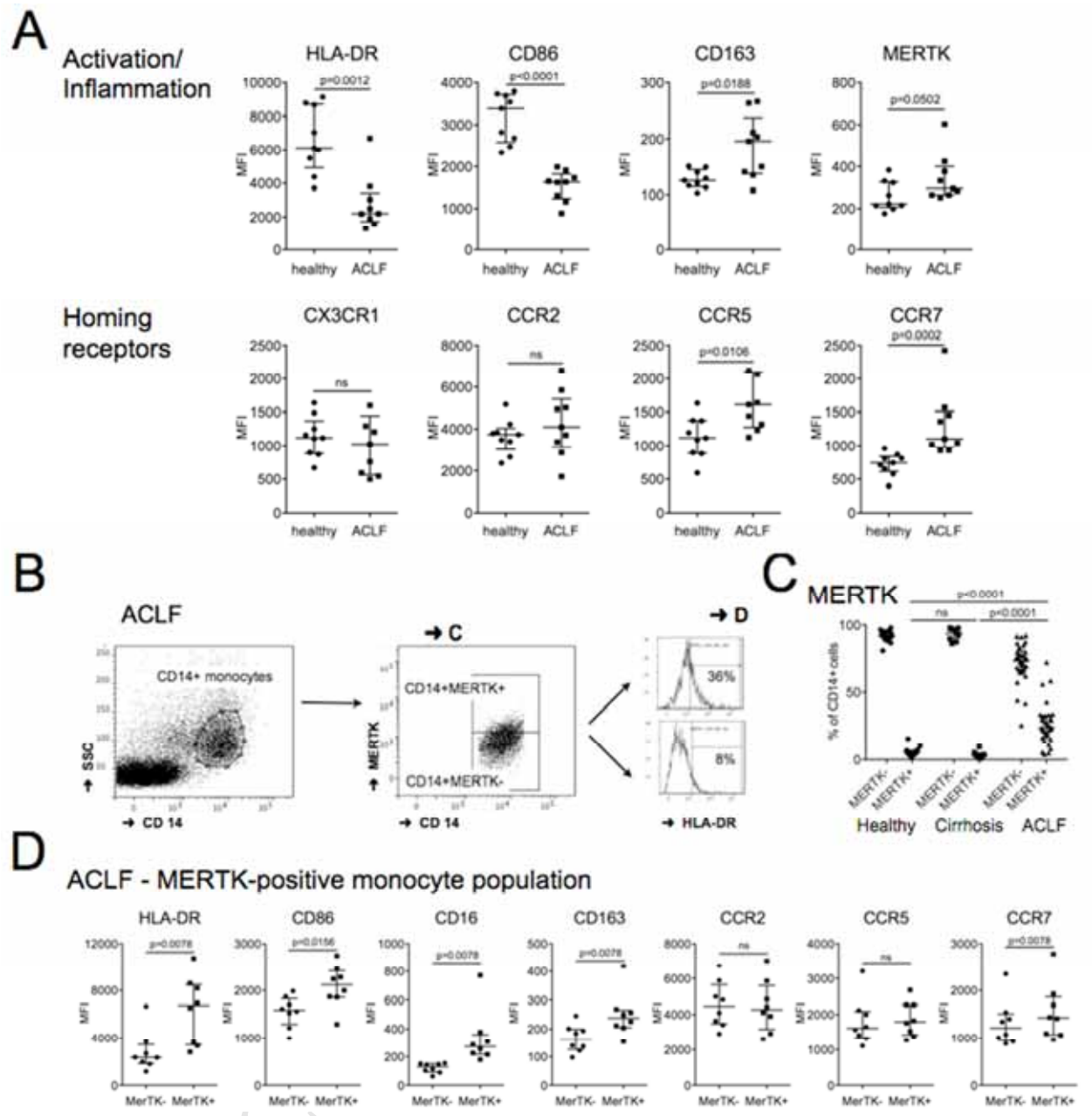
A
Activation/ Inflammation
HLA-DR
p=0.0012
CD86
p<0.0001
CD163
p=0.0188
MERTK
p=0.0502
MFI
healthy
ACLF
Homing receptors
CX3CR1
ns
CCR2
ns
CCR5
p=0.0106
CCR7
p=0.0002
B
ACLF
CD14+ monocytes
SSC
CD 14
C
CD14+MERTK+
CD14+MERTK-
MERTK
CD 14
D
HLA-DR
36%
8%
C
MERTK
p<0.0001
ns
p<0.0001
% of CD14+ cells
MERTK-
MERTK+
Healthy
Cirrhosis
ACLF
D
ACLF - MERTK-positive monocyte population
HLA-DR
p=0.0078
CD86
p=0.0156
CD16
p=0.0078
CD163
p=0.0078
CCR2
ns
CCR5
ns
CCR7
p=0.0078
MFI
MerTK-
MerTK+

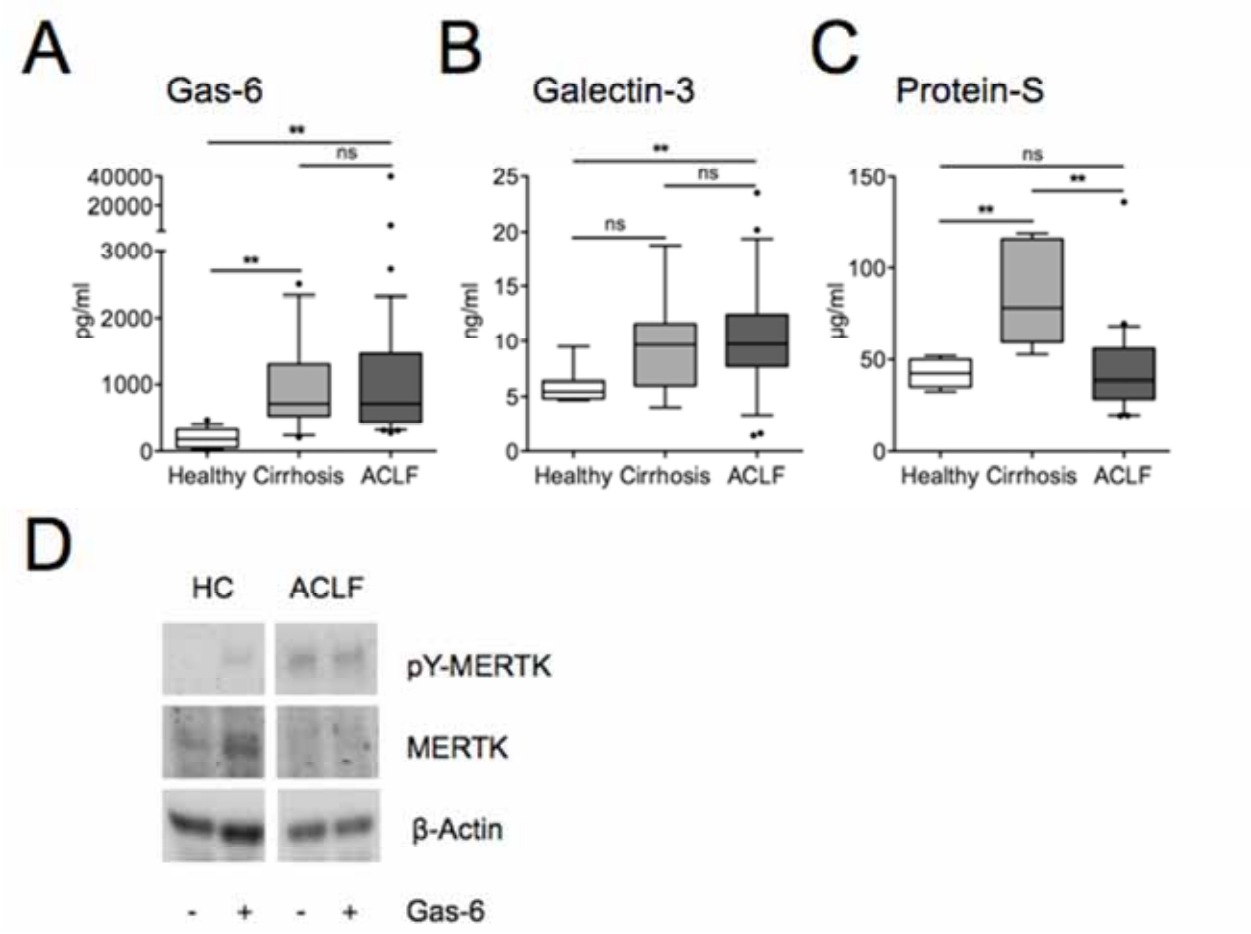
A
Gas-6
pg/ml
40000
20000
3000
2000
1000
0
**
ns
**
Healthy Cirrhosis ACLF
B
Galectin-3
ng/ml
25
20
15
10
5
0
**
ns
ns
Healthy Cirrhosis ACLF
C
Protein-S
μg/ml
150
100
50
0
ns
**
**
Healthy Cirrhosis ACLF
D
HC
ACLF
pY-MERTK
MERTK
β-Actin
- + - +
Gas-6

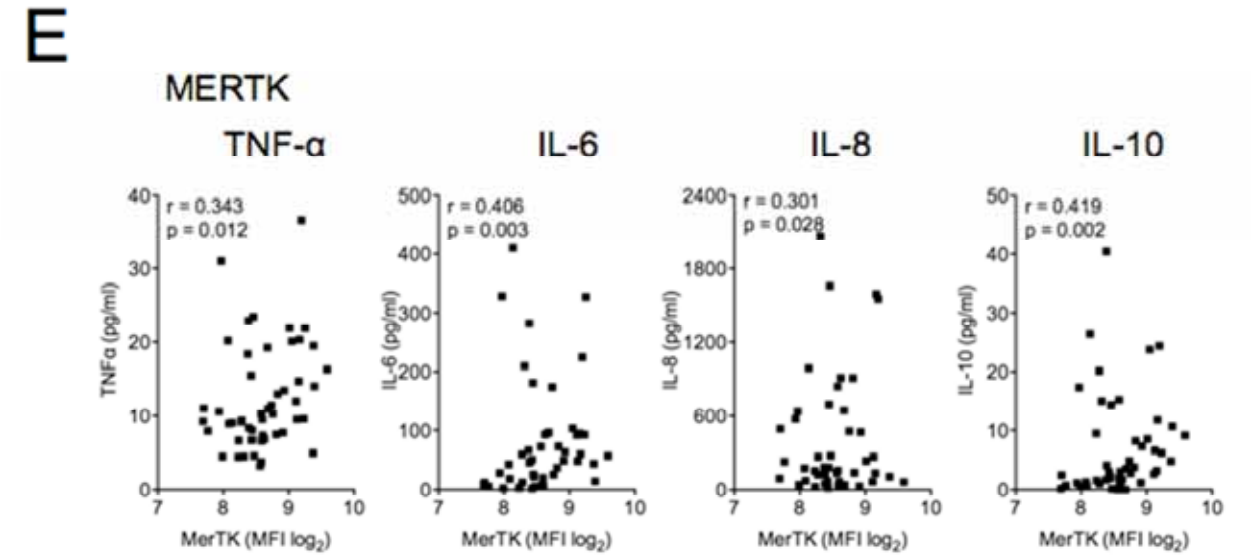
E
MERTK
TNF-α
r = 0.343
p = 0.012
TNFα (pg/ml)
MerTK (MFI log2)
IL-6
r = 0.406
p = 0.003
IL-6 (pg/ml)
MerTK (MFI log2)
IL-8
r = 0.301
p = 0.028
IL-8 (pg/ml)
MerTK (MFI log2)
IL-10
r = 0.419
p = 0.002
IL-10 (pg/ml)
MerTK (MFI log2)

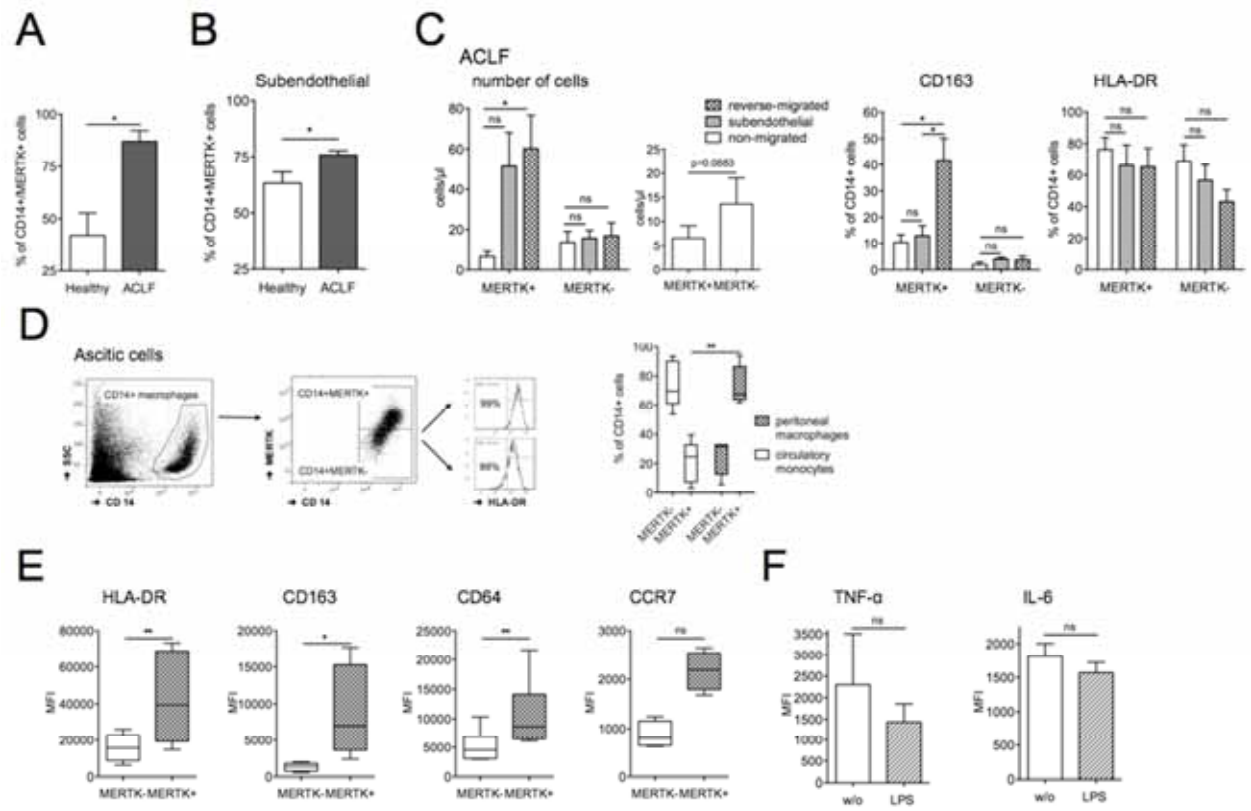

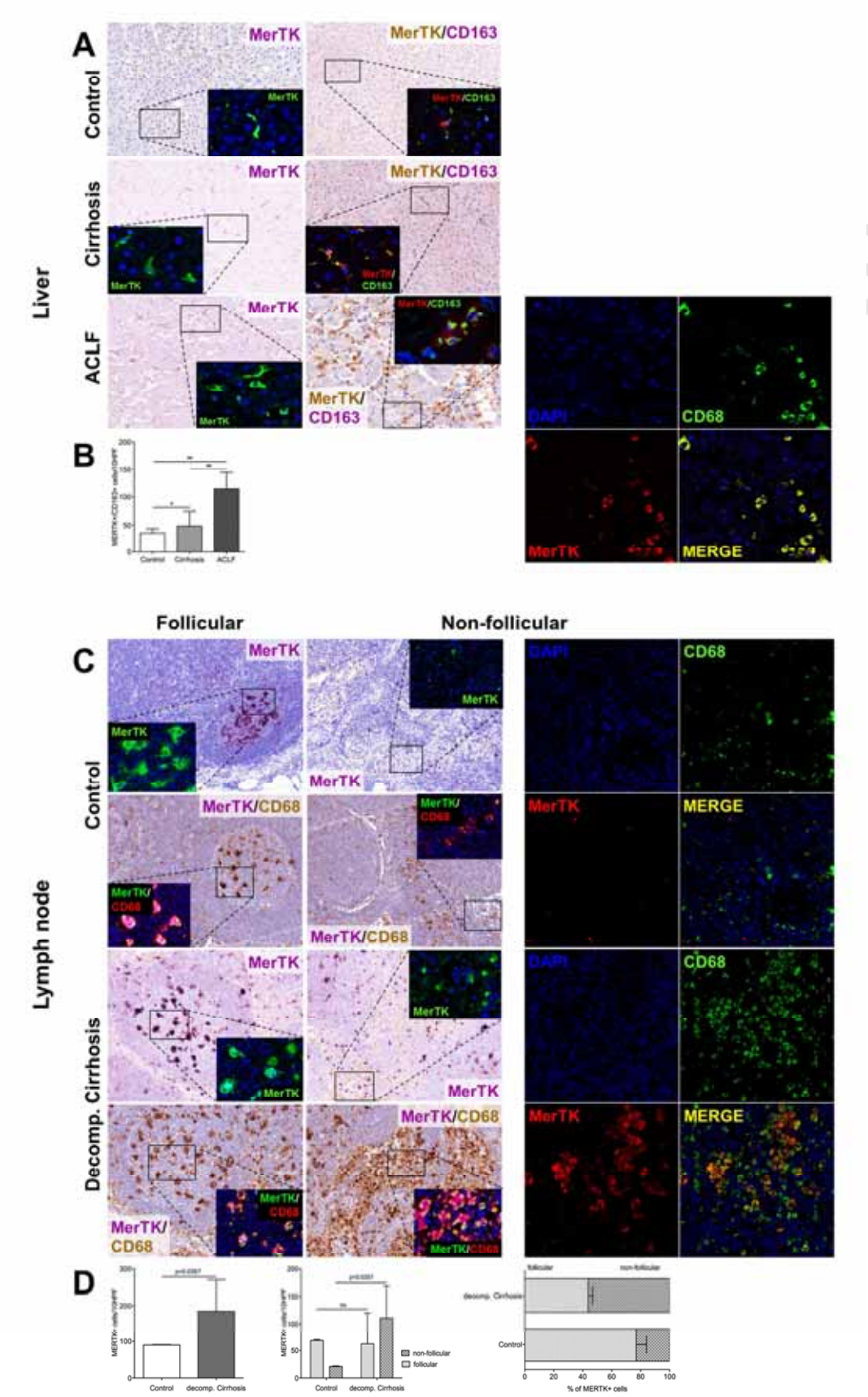
A
Liver
Control
Cirrhosis
ACLF
MerTK
MerTK/CD163
B
Control
Cirrhosis
ACLF
DAPI
CD68
MerTK
MERGE
Follicular
Non-follicular
C
Lymph node
Control
Decomp. Cirrhosis
MerTK/CD68
D
decomp. Cirrhosis
non-follicular
follicular
% of MERTK+ cells

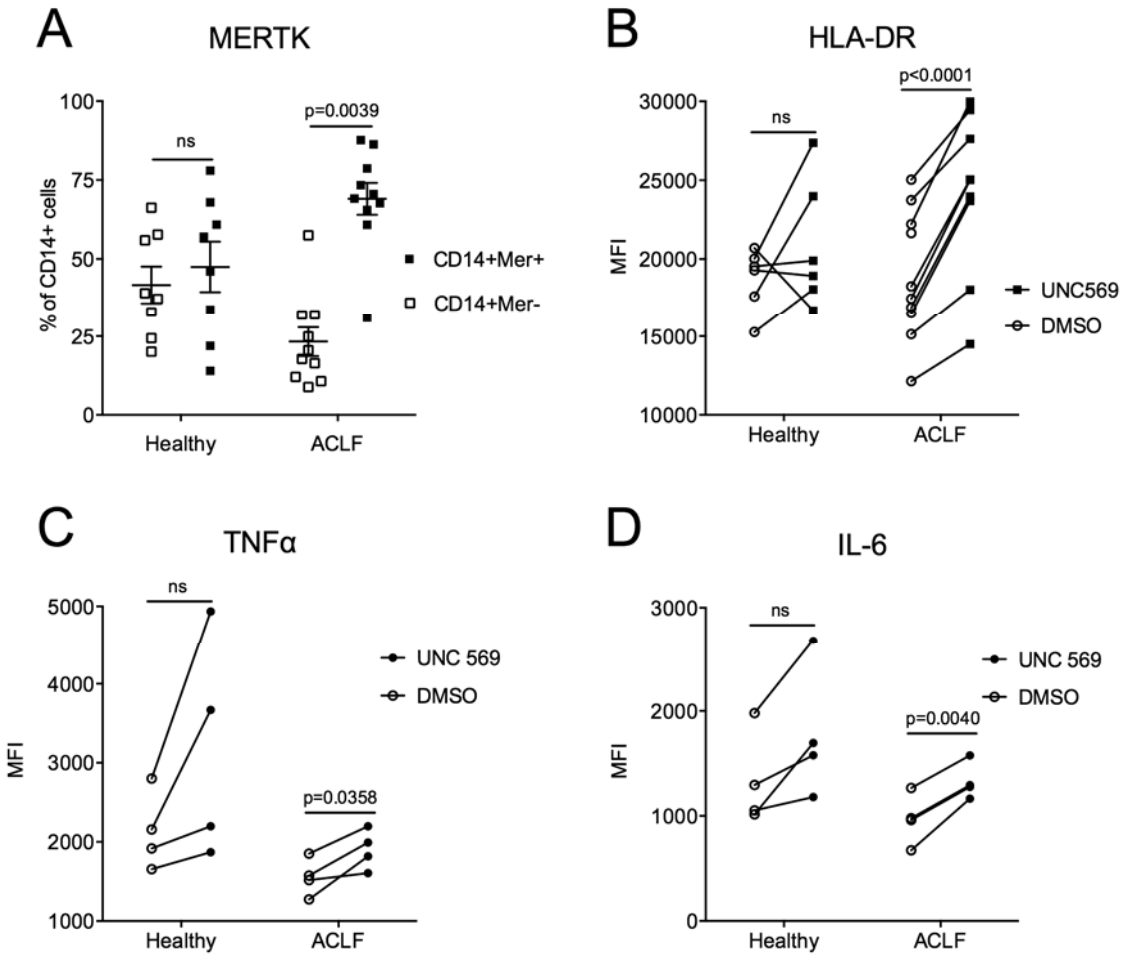
A
MERTK
% of CD14+ cells
100
75
50
25
0
ns
p=0.0039
Healthy
ACLF
CD14+Mer+
CD14+Mer-
B
HLA-DR
MFI
30000
25000
20000
15000
10000
ns
p<0.0001
Healthy
ACLF
UNC569
DMSO
C
TNFα
MFI
5000
4000
3000
2000
1000
ns
p=0.0358
Healthy
ACLF
UNC 569
DMSO
D
IL-6
MFI
3000
2000
1000
0
ns
p=0.0040
Healthy
ACLF
UNC 569
DMSO

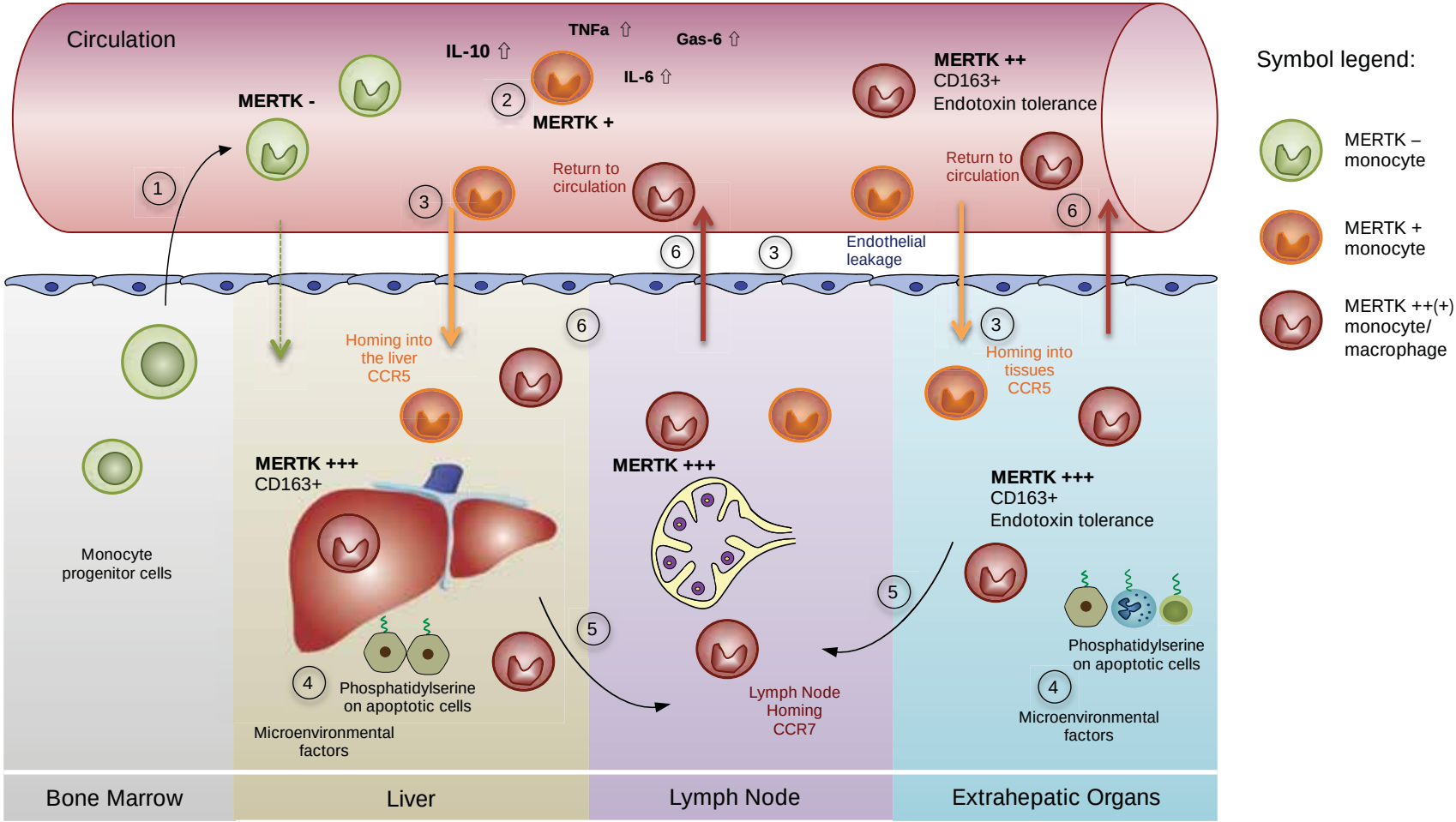
Circulation
TNFa ⇧
IL-10 ⇧
Gas-6 ⇧
IL-6 ⇧
MERTK -
MERTK +
MERTK ++
CD163+
Endotoxin tolerance
Return to circulation
Return to circulation
Endothelial leakage
1
2
3
3
3
4
4
5
5
6
6
6
Homing into the liver
CCR5
Homing into tissues
CCR5
MERTK +++
CD163+
MERTK +++
MERTK +++
CD163+
Endotoxin tolerance
Monocyte progenitor cells
Phosphatidylserine on apoptotic cells
Phosphatidylserine on apoptotic cells
Microenvironmental factors
Microenvironmental factors
Lymph Node Homing
CCR7
Bone Marrow
Liver
Lymph Node
Extrahepatic Organs
Symbol legend:
MERTK – monocyte
MERTK + monocyte
MERTK ++(+) monocyte/ macrophage

Supplementary Material and Methods

Isolation of monocytes

Monocytes were isolated using CD14-microbeads as previously described[1]. To increase the purity of monocytes for protein extraction and Western blotting, we applied a sequence of depletion using CD66abce-, CD56-microbeads and the Pan Monocyte Isolation Kit (Miltenyi Biotec, Germany) according to manufacturer's instructions. Purity of monocyte isolation was assessed by flow-cytometry.

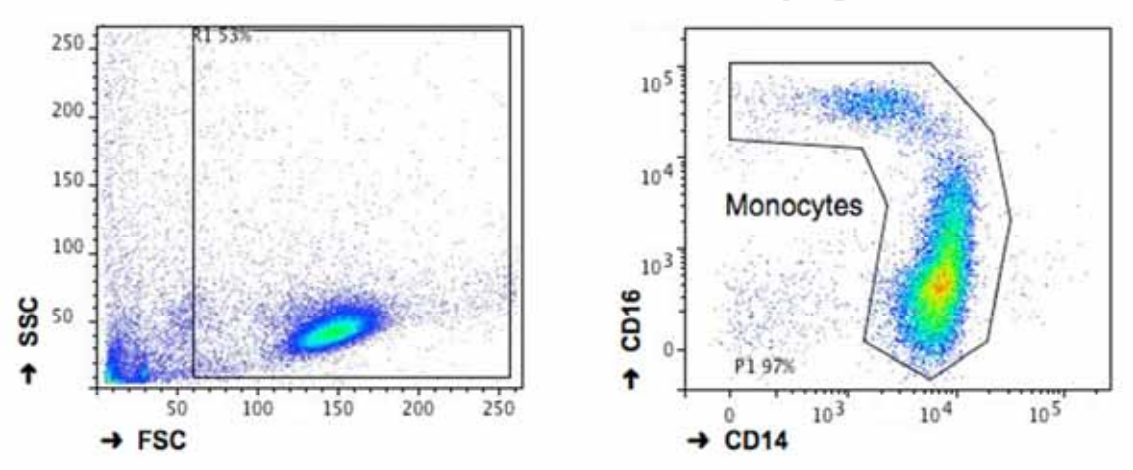

Purity of monocytes following isolation using a sequence of negative selection.

Representative dot plot showing gated monocytes on the forward- and side scatter profile (left). The purity of monocytes including all different subsets was routinely characterised by the expression of CD14 using APC-H7 and CD16 using PerCP-Cy5.5 (a purity of 97% in this representative isolation) (right). SSC: side scatter; FSC: forward scatter.

Migration assay

Cell culture inserts (0.4 μm pore size; Merck Millipore, Germany) were placed in 24-well plates (Corning, USA) containing 700 μl human endothelial-SFM media supplemented with 0.1% BSA (Life Technologies, UK). A collagen plug was then formed in the insert using bovine collagen I (3 mg/ml) prepared with MEM and NaOH, and overlayered with 50 μl human fibronectin (50 μg/ml; Life Technologies, UK). The solutions were then left to equilibrate for 2 h at 37 ℃, 5% CO_2.

Following a further 4-6 h incubation with fresh SFM media, 5×10^4 human umbilical vein endothelial cells (HUVECs) (prepared as described in Jaffe et al.[2]), in EBM-2™ endothelial medium (Lonza, Switzerland), were seeded on top of each collagen plug. HUVECs were grown to confluence for 24 h and then were stimulated with fresh EBM-2™ medium containing TNF-α and IFN-γ (both 10 ng/ml) (R&D Systems) for a further 24 h at 37 ℃, 5% CO_2.

Next, CD14+ microbead-isolated monocytes (Miltenyi Biotec, UK) were pre-conditioned for 24 h with ACLF or HC plasma (20% plasma/complete medium) in 24-well plates. Monocytes, $2x10^6$ in SFM medium, were added on top of the HUVEC/collagen matrix and incubated at 37 ℃, 5% CO_2. After 1.5 h, non-migrated monocytes were harvested by washing thoroughly the top of the well with SFM medium, before fresh (2.5% FBS) SFM medium was added on top. Following a further 24 h incubation at 37 ℃, 5% CO_2, reverse migrated monocytes were harvested by careful aspiration. Subendothelial monocytes were recovered from the HUVEC/collagen matrix by incubation with collagenase solution (Sigma-Aldrich, UK) for 45 min 37 ℃, 5% CO_2. The monocyte populations were then washed with PBS and analysed using a CyAn flow cytometer (Beckman Coulter, UK).

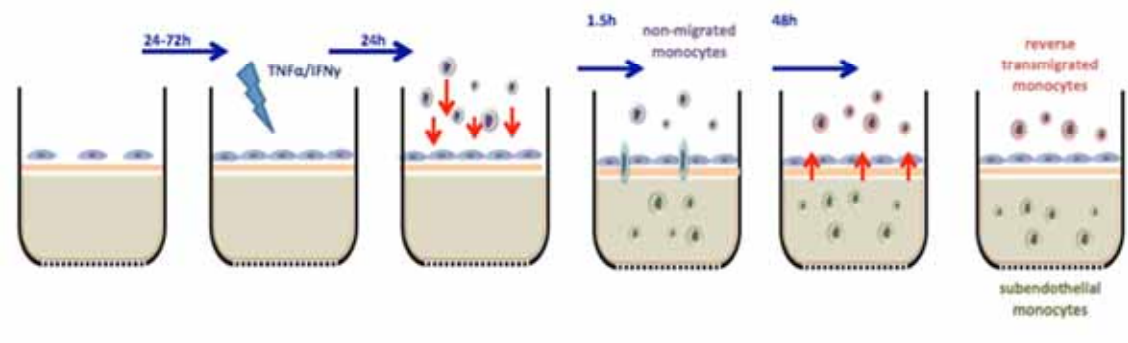

Simplified diagram of the in-vitro migration assay. Endothelial cells are plated on a collagen plug and stimulated with TNF-α/IFN-γ to form a confluent monolayer. Monocytes ($2x10^6$/well) are added on top of the collages plug. Non-migrated monocytes are harvested at 1.5 hours. Following a 24 h culture period, reverse migrated monocytes are harvested and subendothelial monocytes are obtained following collagenase digestion.

Monocyte oxidative burst activity against E.coli

Monocyte intracellular killing of E.coli by oxidative burst was assed using Phagoburst kit (Glycotope, Heidelberg, Germany) following the manufacturer's instructions. Heparinised whole blood from patients with stable cirrhosis, ACLF and healthy controls was processed within maximal 4h after phlebotomy. 100µl of whole blood was incubated with 20µl of E. coli particles for 20 min. at 37℃. Rhodamine was used as a fluorochrome. CD14 positive cells were stained using APC-H7 labeled CD14 antibody for 20 min. The burst activity was immediately assessed by flow cytometry.

Inhibition of MERTK in monocytes in-vitro

For the inhibition of MERTK in-vitro we used the small molecule inhibitor UNC569[3] (Calbiochem Millipore, UK). Monocytes were isolated using CD14 microbeads, purity of monocytes was >90%. Cells were seeded on 48-well plates (500'000 cells/well) and cultured in X-vivo 10 medium (Lonza, Switzerland) containing 25% of plasma from different ACLF patients and HC respectively in a 37℃, 5% CO_2 environment for 16h. Phenotypic analysis using flow-cytometry was performed on these monocytes grown in different donors' plasma.

Cells were treated with UNC569 2 µM or DMSO respectively for 24h prior to phenotypic analysis of HLA-DR expression by flow-cytometry.

For analysis of cytokine production, cells were pre-treated with UNC569 2 µM or DMSO respectively for 2h prior to stimulation with LPS 100 ng/ml for subsequent 4h. TNF-α/ IL-6 production was assessed by flow-cytometry as previously described[1]. Apoptotic cells were stained by Annexin-V (BD Biosciences, UK). UNC569 2 µM had been identified to influence cytokine production as well as HLA-DR expression more potently compared to lower- (1 µM) and higher doses (5 and 10 µM) without increasing the rate of apoptosis to >7%.

To investigate the effect of UNC569 on oxidative burst activity, cells were pre-treated with UNC569 2 µM or DMSO respectively for 2h prior to stimulation with E. coli particles (cell to particle ratio: 250'000 monocytes to 20 µl E. coli) for 20 min at 37℃. Rhodamine was used as a fluorochrome (20 µl per 250'000 cells). CD14 positive cells were stained using APC-H7 labeled CD14 antibody for 20 min. The burst activity was immediately assessed by flow cytometry.

Western Blot for p-Y-MERTK

For protein extraction monocytes isolation from freshly extracted PBMCs was done using the sequential negative selection described above. Purity of monocytes was >95%. Cells were grown on 24-well plates ($2x10^6$ cells/well) in RPMI-1640 medium (Sigma-Aldrich, St. Louis, USA) and starved for 4h. Cells were stimulated with 20 nM human recombinant Gas-6 (R&D systems, UK) or dH_20 respectively for 10 min. The dose was selected in correspondence to the highest plasma level measured in patients with ACLF previously. Cells were harvested on ice and washed in ice-cold PBS containing 1 mmol/l vanadate, centrifuged at 14000 rpm for 5 min. The pellet was lysed in 60µl RIPA buffer (Pierce, Rockford, USA) containing 1 mmol/l vanadate, 1:100 phosphatase inhibitor cocktails 2 and 3 (Sigma-Aldrich, St. Louis, USA) and 1:25 proteinase inhibitor (Roche, Basel, Switzerland) on ice for 30 min. and centrifuged at 14000 rpm for 5 min. Protein concentrations were measured using Bradford reagent (BioRad, Hercules, USA). Samples were denaturated in 4x LDS Sample loading buffer/ 4% β-mercaptoethanol for 5 min. at 100℃. Samples were loaded on a 4-12% NuPAGE Bis-Tris Protein Gel (LifeTechnologies, Paisley, UK), transferred to a PVDF membrane using wet-transfer method (20% methanol) and blocked with 5% milk in PBS-Tween-20 (PBS-T). Antibodies against phospho-Y-MERTK, MERTK and β-actin were obtained from Abcam (Cambridge, UK). For detection 20XLumiGlow/Peroxidase was used (Cell-Signaling, Danvers, USA).

Assessment of sICAM-1 and sVCAM-1

Human soluble intercellular adhesion molecule-1 (hs ICAM-1; ng/ml) and human soluble vascular cell adhesion molecule 1 (hs VCAM-1; ng/ml) were measured by enzyme-linked immunosorbent assay (ELISA) according to manufacturer's instructions (eBioscience, Hatfield, UK).

Immunohistochemistry and confocal microscopy

A. MERTK enzymatic immunohistochemistry

Formalin-fixed and paraffin-embedded (FFPE) tissue was cut at 4 µm using a Leica RM2235 rotary microtome (Leica Biosystems, UK) and picked up on poly-l-lysine coated slides which were manually stained using a rabbit monoclonal anti-MERTK primary antibody (catalog number ab52968, Abcam, UK; dilution 1:300). Slides were dewaxed in xylene, rehydrated, subjected to heat-induced epitope retrieval (HIER) using sodium citrate buffer, pH 6, for 20 minutes, and allowed to cool, followed by 1 hour incubation at room temperature with the primary antibody. The signal was detected using the EnVisionTM G/2 Doublestain System, Rabbit/Mouse (DAB+/Permanent Red) (product number K536111-2, Dako, UK), and visualized with the Vector VIP peroxidase kit (catalog number SH-600, Vector Laboratories, UK). The slides were then dehydrated with alcohol, cleared with xylene and cover slipped with DPX (Leica Biosystems, UK) after hematoxylin counterstaining. Images were captured and processed with a Nikon Eclipse E600 microscope using the Nuance™ 3.0.2 (PerkinElmer, UK) multispectral imaging technology. Cells were counted using ImageJ software (Bethesda, USA) on 10 random high power fields (HPF).

Immunostains were analysed by a liver histopathologist (A.Q.) who was blinded to clinical data.

B. MERTK-CD68 enzymatic immunohistochemistry

FFPE tissue was cut at 4 μm using a Leica RM2235 rotary microtome (Leica Biosystems, UK) and picked up on poly-l-lysine coated slides which were manually stained using a rabbit monoclonal anti-MERTK primary antibody (catalog number ab52968, Abcam, UK; dilution 1:300) and a mouse monoclonal anti-CD68 antibody (product number M0876, Dako, UK; dilution 1:50). Slides were dewaxed in xylene, rehydrated, subjected to heat-induced epitope retrieval (HIER) using sodium citrate buffer, pH 6, for 20 minutes, and allowed to cool, followed by 1 hour incubation at room temperature with the anti-CD68 antibody. The signal was detected using the EnVisionTM G/2 Doublestain System, Rabbit/Mouse (DAB+/Permanent Red) (product number K536111-2, Dako, UK), with 3,3'-diaminobenzidine (DAB) for visualization. The slides were then incubated for 1 hour at room temperature with the anti-MERTK antibody, and the second signal was detected using the same detection kit but with the Vector VIP peroxidase kit (catalog number SH-600, Vector Laboratories, UK) for visualization. Slides were then dehydrated with alcohol, cleared with xylene and cover slipped with DPX (Leica Biosystems, UK) after hematoxylin counterstaining. Images were captured and processed using the same microscope and software as described above.

C. MERTK-CD163 enzymatic immunohistochemistry

FFPE tissue was cut at 4 μm using a Leica RM2235 rotary microtome (Leica Biosystems, UK) and picked up on poly-l-lysine coated slides which were manually

stained using a rabbit monoclonal anti-MERTK primary antibody (catalog number ab52968, Abcam, UK; dilution 1:300) and a mouse monoclonal anti-CD163 antibody (catalog number sc-33715, Santa Cruz Biotechnology, Germany; dilution 1:50). Slides were dewaxed in xylene, rehydrated, subjected to heat-induced epitope retrieval (HIER) using sodium citrate buffer, pH 6, for 20 minutes, and allowed to cool, followed by 1 hour incubation at room temperature with the anti-MERTK antibody. The signal was detected using the EnVisionTM G/2 Doublestain System, Rabbit/Mouse (DAB+/Permanent Red) (product number K536111-2, Dako, UK), with DAB for visualization. Slides were then incubated overnight at 4℃ with the anti-CD163 antibody. The second signal was detected using the Novolink Polymer Detection kit (code RE7200-K, Novocastra, UK) with the Vector VIP peroxidase kit (catalog number SH-600, Vector Laboratories, UK) for visualization. Slides were then dehydrated with alcohol, cleared with xylene and cover slipped with DPX (Leica Biosystems, UK) after hematoxylin counterstaining. Images were captured and processed using the same microscope and software as previously described.

D. MERTK-CD68 fluorescent immunohistochemistry

FFPE tissue was cut at 4 µm using a Leica RM2235 rotary microtome (Leica Biosystems, UK) and picked up on poly-l-lysine coated slides which were manually stained using a rabbit monoclonal anti-MERTK primary antibody (catalog number ab52968, Abcam, UK; dilution 1:100) and a mouse monoclonal anti-CD68 antibody (product number M0876, Dako; UK, dilution 1:100). Slides were dewaxed in xylene, rehydrated, subjected to heat-induced epitope retrieval (HIER) using sodium citrate buffer, pH 6, for 20 minutes, and allowed to cool, followed by an overnight incubation at 4℃ with a cocktail of primary antibodies. The second day the slides were

incubated again overnight in the same conditions with a biotinylated goat-anti rabbit secondary antibody (product number E043201-8, Dako, UK; dilution 1:400) together with an Alexa 488 goat anti-mouse secondary antibody (catalog number A11029, Life Technologies, UK; dilution 1:400). This was followed by a third overnight incubation at 4℃ with Alexa Fluor 548-conjugated s treptavidin (catalog number S-32356, Life Technologies, UK; dilution 1:300). All slides were counterstained with 4′,6-diamidino-2-phenylindole (DAPI) (catalog number D1306, Life Technologies, UK), cover slipped using a fluorescence mounting medium (catalog number S302380-2, Life Technologies, UK) and imaged using a confocal microscope (Zeiss, UK).

E. MERTK-Ki67 enzymatic immunohistochemistry

FFPE tissue was cut at 4 µm using the same rotary microtome as previously specified and picked up on poly-l-lysine coated slides which were manually stained using a rabbit monoclonal anti-MERTK primary antibody (catalog number ab52968, Abcam, UK; dilution 1:300) and a mouse monoclonal anti-Ki67 antibody (product number M7240, Dako, UK; dilution 1:50). Slides were dewaxed in xylene, rehydrated, subjected to heat-induced epitope retrieval (HIER) using sodium citrate buffer, pH 9, for 20 minutes, and allowed to cool, followed by 1 hour incubation at room temperature with the anti-Ki67 antibody. The signal was detected using the EnVisionTM G/2 Doublestain System, Rabbit/Mouse (DAB+/Permanent Red) (product number K536111-2, Dako, UK), with 3,3'-diaminobenzidine (DAB) for visualization. The slides were then incubated for 1 hour at room temperature with the anti-MERTK antibody, and the second signal was detected using the same detection kit but with the Vector VIP peroxidase kit (catalog number SH-600, Vector

Laboratories, UK) for visualization. Slides were then dehydrated with alcohol, cleared with xylene and cover slipped with DPX (Leica Biosystems, UK) after hematoxylin counterstaining. Images were captured and processed using the same microscope and software as described above.

F. MERTK-Ki67 fluorescent immunohistochemistry

FFPE tissue was cut at 4 μm using a Leica RM2235 rotary microtome (Leica Biosystems, UK) and picked up on poly-l-lysine coated slides which were manually stained using a rabbit monoclonal anti-MERTK primary antibody (catalog number ab52968, Abcam, UK; dilution 1:50) and a mouse monoclonal anti-Ki67 antibody (product number M7240, Dako; UK, dilution 1:25). Slides were dewaxed in xylene, rehydrated, subjected to heat-induced epitope retrieval (HIER) using sodium citrate buffer, pH 9, for 20 minutes, and allowed to cool, followed by 1.5 hour incubation at room temperature with a cocktail of primary antibodies. Then the slides were incubated overnight at 4℃ with a mixture of Alexa 488 goat anti-mouse (catalog number A11029, Life Technologies, UK; dilution 1:400) and Alexa Fluor 594 (catalog number A11037, Life Technologies, UK; dilution 1:400). All slides were counterstained with 4′,6-diamidino-2-phenylindole (DAPI) (catalog number D1306, Life Technologies, UK), cover slipped using a fluorescence mounting medium (catalog number S302380-2, Life Technologies, UK) and imaged using a Leica DMR microscope equipped with a Leica DFC300 FX camera using the Leica Application Suite V3.2.0 software (Leica Microsystems, Newcastle Upon Tyne, UK). The images taken for each channel were merged using the ImageJ software (Bethesda, Maryland, USA).

G. Assessing MERTK-expression in macrophages using Nuance multispectral imaging technology and confocal microscopy.

Double epitope enzymatic immunohistochemistry (MERTK-CD68 and MERTK-CD163) was suggestive of co-localisation of MERTK with CD68+ and CD163+in h-mφ. Distinguishing between brown and purple and unmixing these co-localised chromagens are not feasible with an RGB camera as it only uses 3 channels. So a multispectral approach was used on these stains, as well as the MerTK-Ki67 double epitope enzymatic immunohistochemistry. Nuance camera takes several images over different wavelengths, thus identifying the 'individual spectral signature' of each chromagen, saving and unmixing it from adjacent colours. Once unmixed the images are re-coloured to enable distinction of chromogens and inversion to a pseudo-fluorescence image (Figure S7). In addition, confocal examination of double epitope fluorescent immunostains was performed to confirm MERTK expression in macrophages and to overcome a few obstacles such as the thickness of the histological sections, which allowed for the overlapping of signals and the presence of intracellular pigments difficult to distinguish from the DAB visualized signal.

H. Angiopoietin-2 enzymatic immunohistochemistry

Explanted liver tissue was obtained in 6 patients undergoing orthotopic liver transplantation (OLT) due to cirrhosis, and 5 undergoing the same procedure for ACLF. Hepatic resection margins of colorectal malignancies (4 cases) served as normal control tissue. Tissue samples were taken for diagnostic histological examination and were formalin-fixed and paraffin-embedded. Angiopoietin-2 (Ang-2)

expression was assessed using the ImageJ software (Bethesda, Maryland, USA) on 10 random high power fields (HPF) from portal tracts in the control group and fibrous septa in the cirrhosis and ACLF groups, as well as from hepatic plates in all three groups. Immunostains were analyzed by a liver histopathologist (A.Q.) who was blinded to clinical data.

FFPE tissue was cut at 4µm using a Leica RM2235 rotary microtome (Leica Biosystems, UK) and picked up on poly-l-lysine coated slides which were manually stained using a mouse monoclonal anti-Ang-2 primary antibody (catalog number sc-74403, Santa Cruz Biotechnology, Germany; dilution 1:50). Slides were dewaxed in xylene, rehydrated, subjected to heat-induced epitope retrieval (HIER) using Tris-EDTA, pH 9, for 20 minutes, and allowed to cool, followed by 1h incubation at room temperature with the primary antibody. The signal was detected using the Novolink Polymer Detection kit (code RE7200-K, Novocastra, Newcastle, UK), and visualized with 3,3'-diaminobenzidine (DAB) (code 4065, Dako, Cambridgeshire, UK). The slides were then dehydrated with alcohol, cleared with xylene and cover slipped with DPX (Leica Biosystems, UK) after hematoxylin counterstaining. Sections were imaged with a Leica DM6000 B microscope (Leica Biosystems, Newcastle, UK) equipped with a Leica DFC300 FX camera (Leica Biosystems, Newcastle, UK). Images were captured and archived using the Leica Laser Microdisection LMD software, version 6.7.0.3754 (Leica Biosystems, Newcastle, UK).

Random HPF (400 ×) were selected as follows: 10 HPF containing portal tracts and 10 HPF from hepatic plates in the control group; 10 HPF from fibrous septa and 10 HPF from hepatic plates in the Cirrhosis and ACLF groups. After software calibration using a grid embedded in the image, the regions of interest (ROI) from each image were selected as follows: portal tracts and fibrous septa within each HPF. Their

areas were measured using the *Freehand Selection* tool and the *Measure* command from the *Analyze* menu. In the case of HPF from hepatic plates, the area of the entire HPF was measured using the same tools. Tissue areas outside the ROIs were excluded using the *Clear Outside* tool from the *Control Panel* menu. Images were then converted to RGB stacks (*Image→Type→RGB Stack*) and the Blue channel was selected for signal analysis. After adjusting the threshold (*Image→Adjust→Threshold*), the area of the Ang-2 signal was assessed using the Measure command. Results were expressed as percentage of Ang-2 signal within the ROI.

References

1. Antoniades CG, Khamri W, Abeles RD, et al. Secretory leukocyte protease inhibitor: a pivotal mediator of anti-inflammatory responses in acetaminophen-induced acute liver failure. Hepatol. Baltim. Md 2014;59:1564–1576.

2. Jaffe EA, Nachman RL, Becker CG, et al. Culture of human endothelial cells derived from umbilical veins. Identification by morphologic and immunologic criteria. J. Clin. Invest. 1973;52:2745–2756.

3. Christoph S, Deryckere D, Schlegel J, et al. UNC569, a novel small-molecule mer inhibitor with efficacy against acute lymphoblastic leukemia in vitro and in vivo. Mol. Cancer Ther. 2013;12:2367–2377.

Table S1

Parameter	Cirrhosis			Acute	ACLF	ALF
	Child A-C	Child A	Child B/C	(AD)		
	(n=17)	(n=7)	(n=10)	(n=9)	(n=41)	(n=23)
Age (years)	55 (47-63)	60 (55-67)	52 (36-60)	50 (42-64)	48 (37-57)	35 (26-47)
Child-Pugh	8 (6-9)	6 (6-6)	9 (8-10)	11 (10-13)	12 (11-13) ‡§	13 (11-13)
MELD	11 (8-16)	9 (7-11)	16 (11-17)	17 (14-29)	33 (25-39) ‡§	38 (33-40)
CLIF-SOFA	3 (1.5-5)	3 (0-3)	4.5 (3-5)	8 (7-10)	14 (12-17) ‡§	-
NACSELD	0	0	0	0	2 (1-3) ‡§	-
SOFA	NA	NA	NA	10.5 (8.3-12.8)*	13 (11.3-14.8)	12 (8-15)
APACHE II	NA	NA	NA	20 (16.8-22.5)*	23 (19-26)	19 (11-24)
SAPS II	NA	NA	NA	28 (22.3-32.3)*	36 (27.3-43-5)	37 (24-48)
Bilirubin (µmol/l)	29 (16.5-72)	23 (11-28)	58 (25-98)	178 (39-309.5)	140 (83.5-328.5) ‡	92 (53-193)

INR	1.3 (1.2-1.6)	1.3 (1.0-1.4)	1.4 (1.2-1.8)	2.1 (1.7-2.6)	2.0 (1.7-2.9) ‡	4.57 (2.69-8.39)
ASAT (U/l)	50 (31.5-99)	46 (25-55)	75 (32-159)	73 (47-461)	115 (72-298.5) ‡	3255 (865-6674)
Lactate (mmol/l)	1.8 (1.3-2.4)	1.6 (1.3-2.2)	NA	1.7 (1.0-2.1)	1.8 (1.2-2.9)	2.9 (2.2-4.9)
pH	7.39 (7.38-7.41)	7.38 (7.38-7.40)	7.43 (7.41-7.44)	7.44 (7.42-7.46)	7.40 (7.34-7.44)	7.41 (7.37-7.45)
WBC (x10e9/l)	4.8 (3.7-6.9)	4.5 (4.1-5.5)	5.7 (3.2-7.9)	6.5 (2.3-12.4)	11.1 (6.3-14.6) ‡	10.53 (8.13-16.29)
Monocytes (x10e9/l)	0.41 (0.27-0.52)	0.36 (0.25-0.46)	0.47 (0.25-0.62)	0.52 (0.18-0.86)	0.52 (0.33-0.86) ‡	0.36 (0.17-0.73)
CRP (mg/dl)	8.5 (3.8-27.0)	5.5 (2.5-9.2)	35.8 (18.1-53.7)	20.2 (9.3-94.1)	52.2 (33.7-78.3) ‡	17.1 (4.5-41.1)
SIRS score	0 (0-1)	0 (0-1)	0 (0-1)	1 (1-1.5)	2 (1-2) ‡	2 (1-3)
Variceal bleed at admission n (%)	0 (0%)	-	-	2 (22.2%)	16 (39.0%)	0 (0%)
Suspected infection at admission n (%)	0 (0%)	-	-	3 (33.3%)	13 (31.7%)	1 (4.4%)
Culture positive infection at admission n (%)	0 (0%)	-	-	2 (22.2%)	3 (7.3%)	2 (8.7%)
Secondary infectious complications n (%)	0 (0%)	-	-	1 (11.1%)	14 (34.1%)	5 (21.7%)

Corticosteroid treatment at admission n (%)	0 (0%)	-	-	1 (11.1%)**	17 (41.5%)***	4 (17.4%)***
Antibiotic treatment at admission n (%)	0 (0%)	-	-	8 (88.8%)	37 (90.2%)	22 (95.7%)

Table S1. Disease severity scores and clinical parameters and characteristics for the different groups of patients with cirrhosis and ACLF. Clinical characteristics and calculated disease severity scores for the different groups of patients at the time of blood sampling and experimental ex-vivo assays. Data are expressed as medians (IQR). Differences were calculated using Mann-Whitney tests. Culture positive infectious complications at admission and with 14 days after admission (secondary infections) for AD or ACLF. Data are expressed as number and % of patients. Cause for ACLF: infection (n=13[32%]; gastrointestinal bleeding n=16[39%]; other n=4[10%]; unknown n=8[20%]; Cause for AD: infection n=3[33%]; gastrointestinal bleeding n=2[22%]; other n=3[33%]; unknown n=1[11%];

NA, not applicable/available. Ns, not statistically significant ($p \geq 0.05$). ‡ significant difference comparing patients with ACLF to cirrhosis (Child-Pugh A-C); § significant difference comparing patients with ACLF to acute decompensated patients (AD); * applicable for AD patients admitted to intensive care only; ** for autoimmune hepatitis; *** for autoimmune disease or suspected relative adrenal insufficiency;

ACLF, acute on chronic liver failure; MELD, model of end-stage liver disease; SOFA, Sequential Organ Failure Assessment score; CLIF, Consortium on Chronic Liver Failure; APACHE II, Acute Physiology and Chronic Health Evaluation II; SAPS II, Simplified Acute Physiology Score II; NACSELD, North American Consortium for Study of End-stage Liver Disease; INR, international normalised ratio; ASAT, aspartate aminotransaminase; WBC, white blood cells; CRP C-reactive protein; SIRS, Systemic inflammatory response syndrome.

Supplementary Figure Legends

Figure S1. MERTK expressing macrophages accumulate in the liver and in mesenteric lymph nodes but not the bone marrow in patients with ACLF and decompensated cirrhosis. A. Representative confocal images of double-epitope fluorescent immunostaining for CD68(green)/MERTK(red)/co-localization(yellow) in explanted liver tissue from control- (upper panel) and cirrhosis patients (lower panel), and follicular areas of regional lymph nodes from control (upper panel) and decompensated cirrhosis (lower panel) (400× magnification). B. Representative single-epitope immunostaining for MERTK (purple) in bone marrow tissue from a decompensated cirrhotic patient (upper left panel); representative composite pseudofluorescent images of MERTK-Ki67 double-epitope immunostaining in liver tissue from control (upper right), cirrhosis (lower left) and ACLF patients (lower right) (200×). C. Representative micrographs of double-epitope fluorescent staining for MERTK-Ki67 in non-follicular areas of lymph nodes from control- and decompensated cirrhotic patients (400×). D. Representative example of Nuance multispectral imaging used to determine MERTK/CD163 co-localisation in ACLF explanted liver tissue: double-epitope immunostaining demonstrating MERTK+(brown)/CD163+(purple) cells (200×); pseudofluorescent image of MERTK+(green), CD163+(red) cells following the unmixing process and co-localisation (yellow).

Figure S2. Representative FACS plot for ex-vivo MERTK staining on monocytes in fresh whole blood. Whole blood from a healthy control compared to an ACLF patient was stained within 2 hours of sampling to assess monocyte MERTK

expression by flow-cytometry. Monocytes in ACLF were predominantly CD14+ (>95%) and MERTK expression was highest in the CD14+CD16+ monocyte population.

Figure S3. MERTK expression on monocytes, Gas-6- and Galectin-3 levels in ACLF do not differ between aetiologies of chronic liver disease. A. MERTK expression on monocytes assessed by flow-cytometry is expressed as mean fluorescence intensity (MFI). B. Gas-6 levels (pg/ml) and C. Galectin-3 levels (ng/ml) were assessed by ELISA. Values were separated by aetiology of liver disease. ACLF patients (n=41): alcoholic liver disease (ALD) (n=19), non-alcoholic fatty liver disease (NAFLD) (n=6), hepatitis C virus infection (HCV) (n=1), autoimmune hepatitis (AIH) (n=3), cholestatic liver disease (n=2), alpha1-antitrypsin deficiency (A1AT) (n=3), and rare diseases such as hereditary haemochromatosis (HHC) (n=1), Wilson's disease (n=1), nodular regenerative hyperplasia (NRH) (n=1), Alagille's syndrome (n=1), chronic Budd-Chiari (n=1), cryptogenic cirrhosis (n=1). Graphs show median/IQR if applicable. Differences between groups of disease of n≥2 were calculated by Mann-Whitney tests; there were no significant differences detected.

Figure S4. MERTK expression is related to SIRS response and liver disease severity. A. MERTK expression on monocytes (MFI) in ACLF/AD patients with no SIRS (SIRS score 0-1) vs. SIRS (SIRS score 2-4). B. MERTK expression in patients with no SIRS and SIRS with and without culture positive infection (no SIRS – no infection n=22; no SIRS – infection n=7; SIRS – no infection n=9; SIRS – infection n=9). C. MERTK expression in relation to the aetiology of decompensation. D. MERTK expression on monocytes in correlation to the leucocyte count (x10e9/l) and

plasma CRP level (mg/l). E. MERTK expression in relation to antibiotic treatment at baseline (n=3 without antibiotics; n=37 on broad spectrum antibiotics). F. Steroid treatment at admission in relation to liver disease severity scores MELD, CLIF-SOFA and MERTK expression (without steroids [w/o] n=23; on steroid treatment for autoimmune disease or clinically suspected relative adrenal insufficiency n=17). Mann-Whitney tests.

Figure S5. Bacterial killing is preserved in acute on chronic liver failure. Monocyte intracellular killing of E.coli by oxidative burst was investigated ex-vivo in whole blood samples. A. Representative FACS plot showing oxidative burst activity (% CD14+ cells) in a healthy control and a patient with ACLF. B. Monocyte oxidative burst in patients with ACLF (n=34) and cirrhosis (n=11) and compared to healthy controls (n=23). C. Oxidative burst activity in patients with ACLF and different outcome: 28-day survival (good; n=12), patients undergoing OLT within 28 days (n=5) and non-survivors (n=17). D. Ex-vivo oxidative burst activity in ACLF patients followed over 14 days after admission (BL, baseline, day 3-5, day 7-10, day 14). E. Fcγ-receptor expression (CD64, CD32) on monocytes from ACLF patients and healthy controls ex-vivo (n=9 each). F. Oxidative burst in response to E.coli after conditioning of healthy monocytes in ACLF- compared to healthy plasma in-vitro (% CD14+ cells) (left) and oxidative burst in response to E.coli after treatment with UNC569 (2µM) for 2h (n=4 each; right).

Figure S6. Systemic cytokine levels in ACLF patients. A-G. A panel of different cytokines was measured in the plasma of patients with ACLF (n=43) compared to stable cirrhosis (n=17) and healthy controls (n=20). TNF-α (A), IL-6 (B), IL-10 (C), IL-

8 (D), IFN-γ (E), TGF-β1 (F), IL-1β (G), IL-12 (H). Data are expressed as pg/ml and represented as box-plots. Differences were calculated using Mann-Whitney tests.

Figure S7. Healthy monocytes cultured in ACLF plasma differentiate towards a MERTK expressing, immunomodulatory population. Healthy monocytes were cultured in medium containing ACLF plasma from different donors (n=10) compared to healthy plasma (n=2) for 36h. Differential expression of cell surface markers after conditioning in different plasma was assessed by flow-cytometry: MERTK, CD16, HLA-DR, CD86, CD163, CD64, CD32, CX3CR1, CCR5, CCR7. Data are expressed as MFI. Graphs show median/IQR.

Figure S8. Inhibition of pro-inflammatory cytokine production in response to LPS-challenge in monocytes cultured in ACLF plasma. Healthy monocytes conditioned with ACLF plasma for 36h were stimulated with LPS (100ng/ml) and TNF-α (A) and IL-6 (B) secretion were measured in cell culture supernatants by ELISA. Levels are expressed in pg/ml of media.

Figure S9. MERTK expression in relation to coagulation and markers of endothelial activation. A. MERTK expression on monocytes in CLD (MFI) is positively correlated to INR but not platelets. B. Markers of endothelial activation (human soluble intercellular adhesion molecule-1 (hs ICAM-1; ng/ml) and human soluble vascular cell adhesion molecule 1 (hs VCAM-1; ng/ml) are elevated in patients with cirrhosis (n=8) and ACLF (n=24) compared to healthy controls (n=8). MERTK expression on monocytes did correlate with neither hs ICAM-1 (Spearman

r=0.200; ns) nor hs VCAM-1 (r=-0.079; ns). C. Representative single epitope immunohistochemistry for Angiopoitin-2 (Ang-2) in cases from the control, cirrhosis and ACLF groups (100× magnification) showing little expression in sinusoids in all groups, and increased endothelial expression in vessels from fibrous septa in cirrhosis and ACLF compared to the controls. Percentage of Ang-2 signal within regions of interest in all three groups (Control n=4; cirrhosis n=6, ACLF n=5).

Figure S10. Phenotypic differentiation of peritoneal macrophages in comparison with circulatory monocyte ex-vivo. Paired samples of peripheral blood and ascites were obtained from n=5 patient with cirrhosis complicated by ascites. Cell surface marker expression of HLA-DR, CD163, CD64, CX3CR1, CCR5, and CCR7 was assessed by flow-cytometry and compared between circulatory monocytes and peritoneal macrophages (pMφ). Data are expressed as MFI and represented as box-plots.

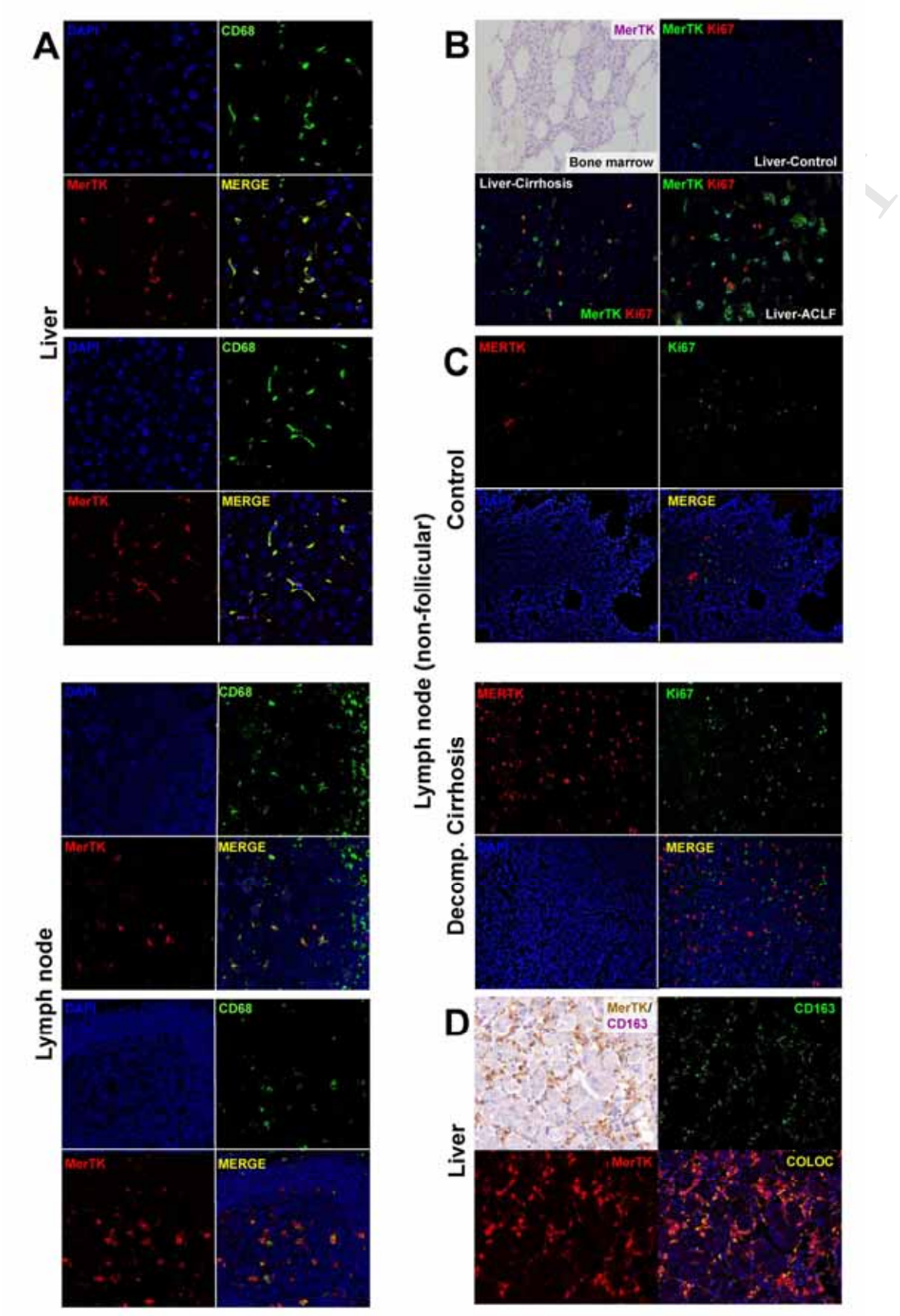
A
Liver
DAPI
CD68
MerTK
MERGE
DAPI
CD68
MerTK
MERGE
Lymph node
DAPI
CD68
MerTK
MERGE
DAPI
CD68
MerTK
MERGE
B
MerTK
Bone marrow
MerTK Ki67
Liver-Control
Liver-Cirrhosis
MerTK Ki67
MerTK Ki67
Liver-ACLF
C
Lymph node (non-follicular)
Control
MERTK
Ki67
DAPI
MERGE
Decomp. Cirrhosis
MERTK
Ki67
DAPI
MERGE
D
Liver
MerTK/
CD163
CD163
MerTK
COLOC

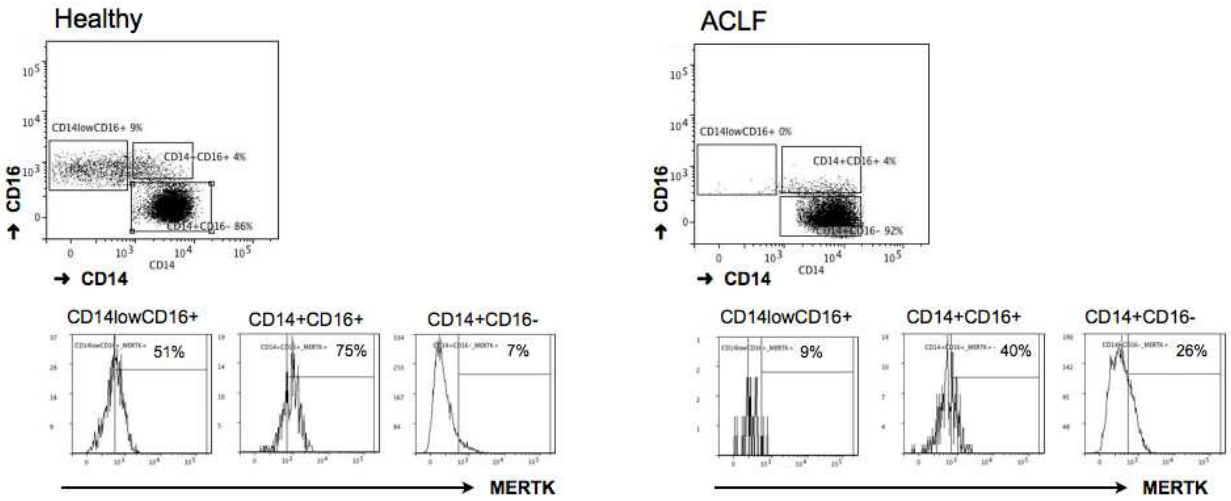

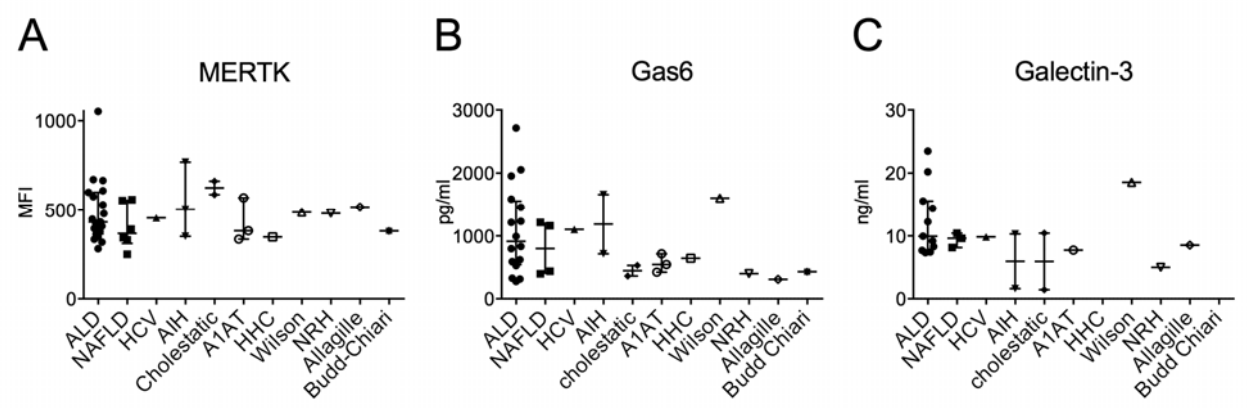

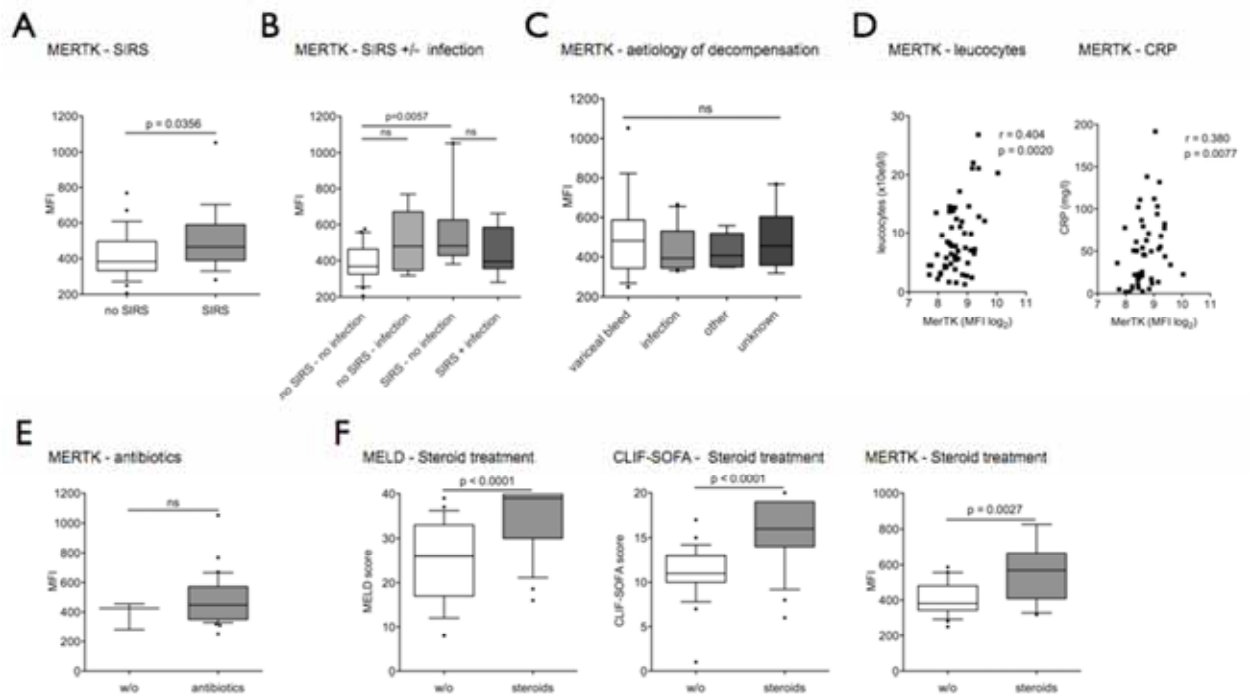

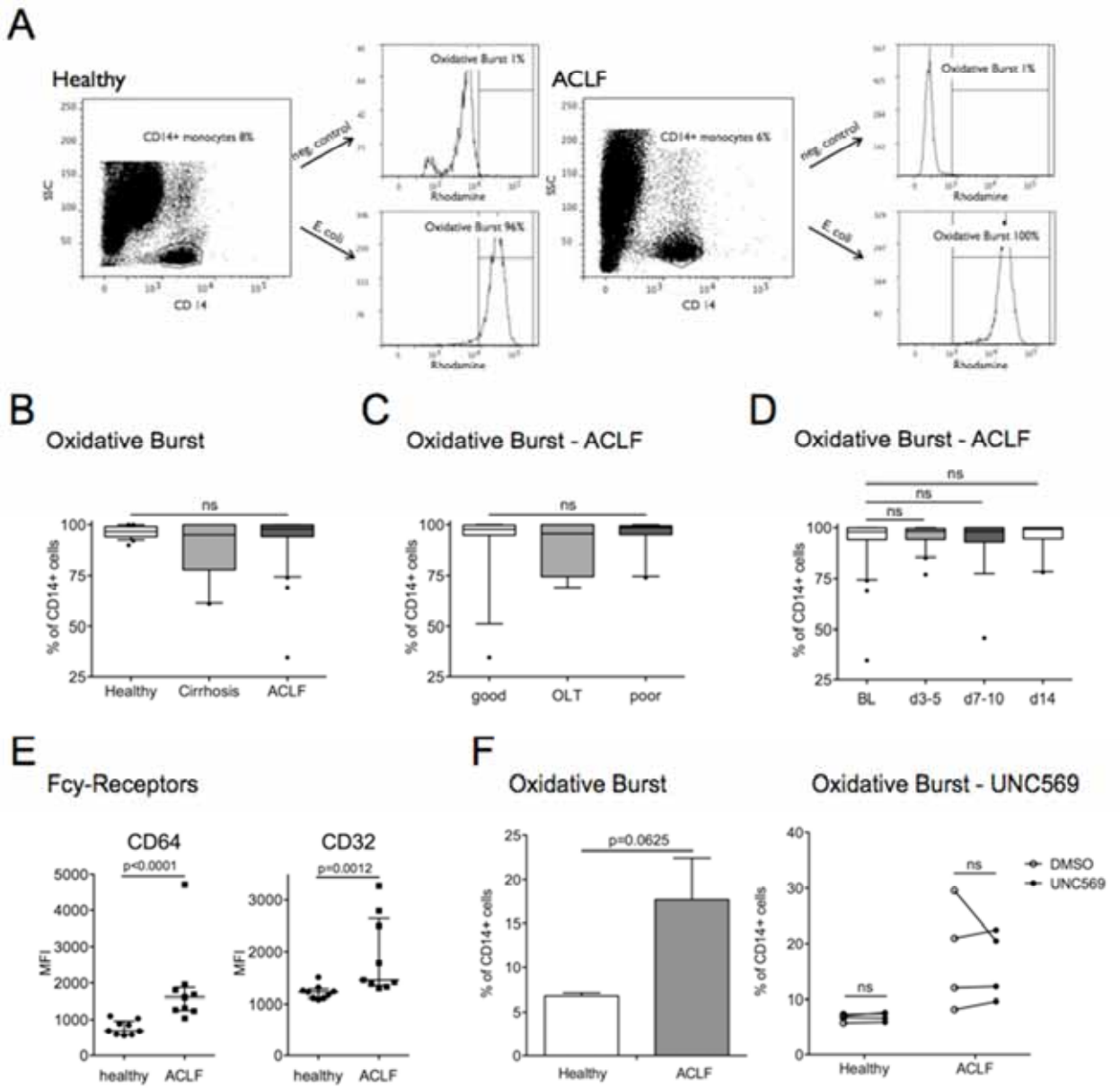
A
Healthy
CD14+ monocytes 8%
SSC
CD 14
neg. control
E. coli
Oxidative Burst 1%
Oxidative Burst 96%
Rhodamine
ACLF
CD14+ monocytes 6%
Oxidative Burst 1%
Oxidative Burst 100%
B
Oxidative Burst
% of CD14+ cells
ns
Healthy
Cirrhosis
ACLF
C
Oxidative Burst - ACLF
good
OLT
poor
D
Oxidative Burst - ACLF
BL
d3-5
d7-10
d14
E
Fcy-Receptors
CD64
p<0.0001
MFI
healthy
ACLF
CD32
p=0.0012
F
Oxidative Burst
p=0.0625
Oxidative Burst - UNC569
DMSO
UNC569

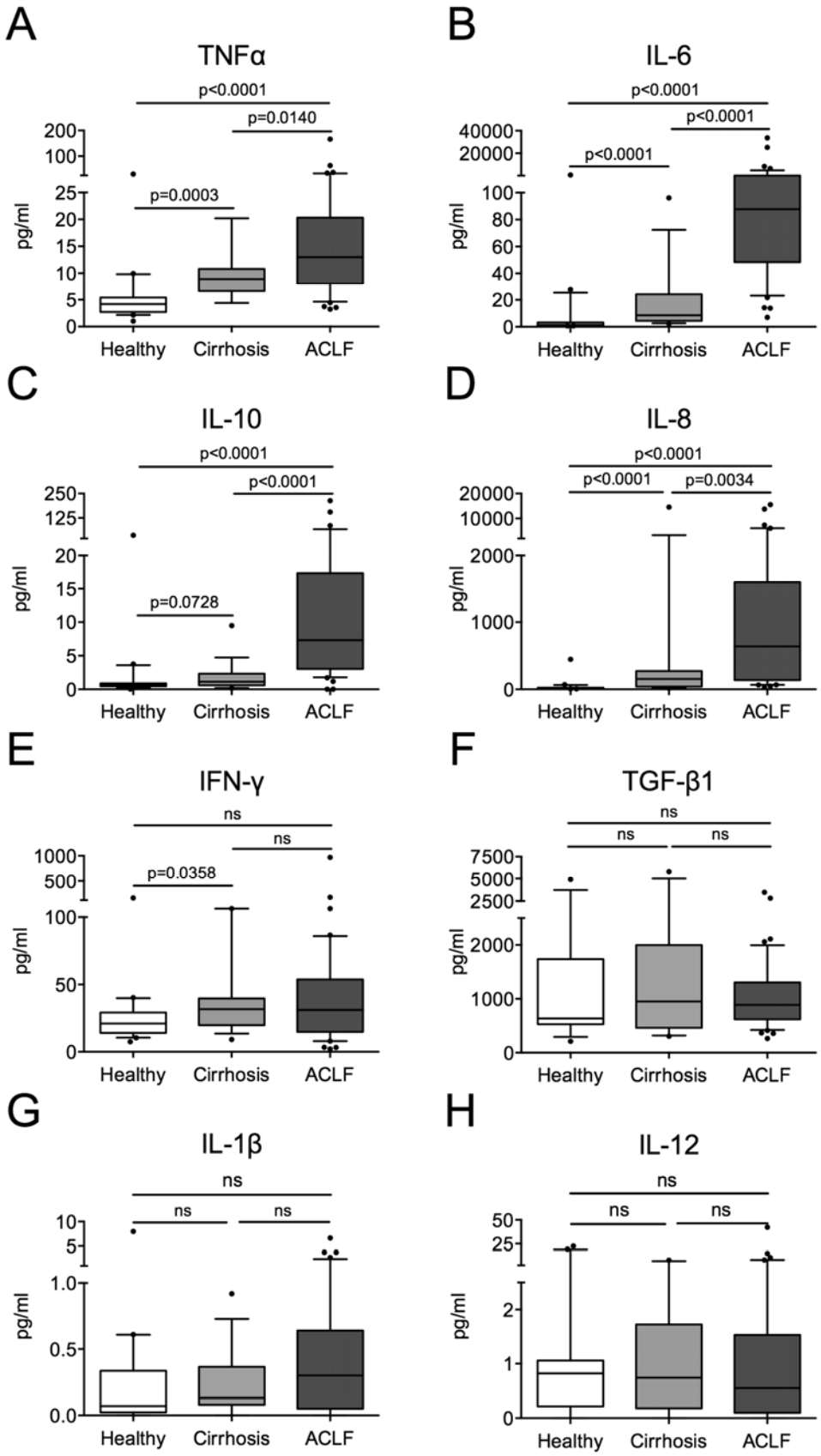
A
TNFα
p<0.0001
p=0.0140
p=0.0003
pg/ml
200
100
25
20
15
10
5
0
Healthy
Cirrhosis
ACLF
B
IL-6
p<0.0001
p<0.0001
p<0.0001
pg/ml
40000
20000
100
80
60
40
20
0
Healthy
Cirrhosis
ACLF
C
IL-10
p<0.0001
p<0.0001
p=0.0728
pg/ml
250
125
20
15
10
5
0
Healthy
Cirrhosis
ACLF
D
IL-8
p<0.0001
p<0.0001
p=0.0034
pg/ml
20000
10000
2000
1000
0
Healthy
Cirrhosis
ACLF
E
IFN-γ
ns
ns
p=0.0358
pg/ml
1000
500
100
50
0
Healthy
Cirrhosis
ACLF
F
TGF-β1
ns
ns
ns
pg/ml
7500
5000
2500
2000
1000
0
Healthy
Cirrhosis
ACLF
G
IL-1β
ns
ns
ns
pg/ml
10
5
1.0
0.5
0.0
Healthy
Cirrhosis
ACLF
H
IL-12
ns
ns
ns
pg/ml
50
25
2
1
0
Healthy
Cirrhosis
ACLF

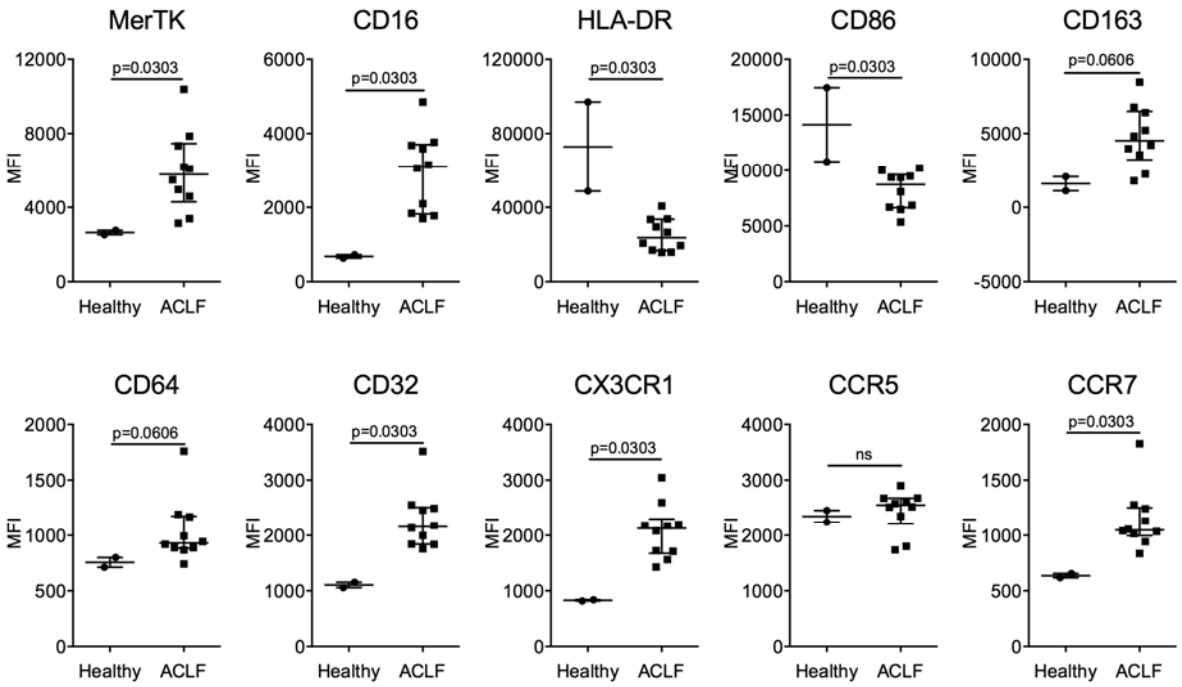

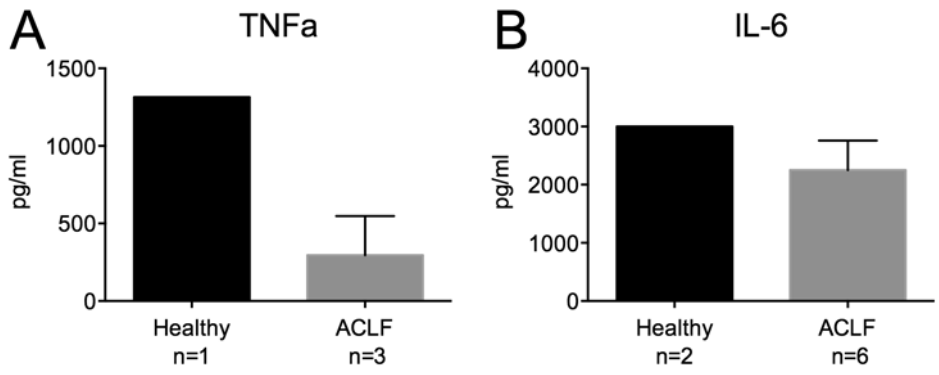

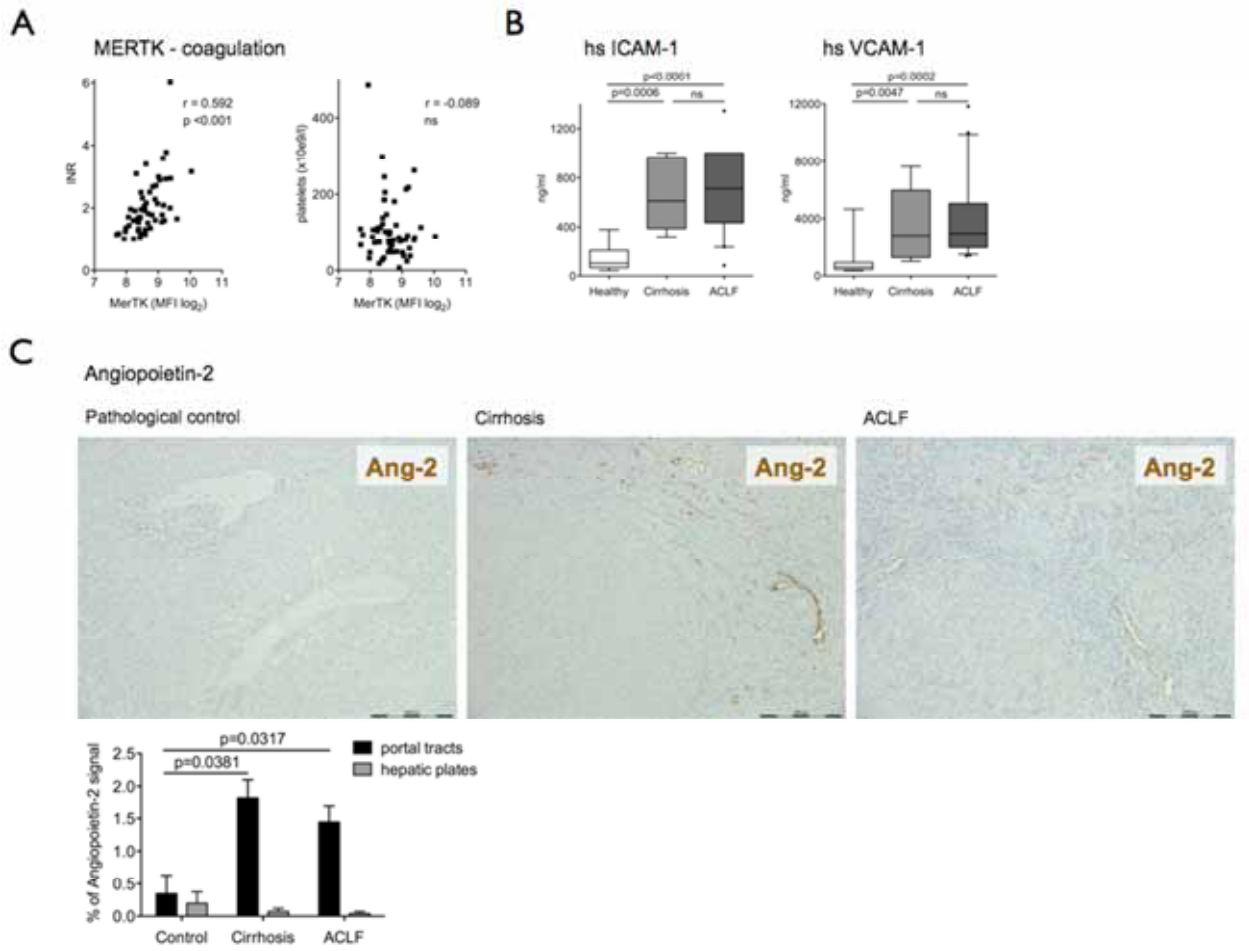
A
MERTK - coagulation
r = 0.592
p <0.001
INR
MerTK (MFI log2)
r = -0.089
ns
platelets (x10e9/l)
MerTK (MFI log2)
B
hs ICAM-1
p<0.0001
p=0.0006
ns
ng/ml
Healthy
Cirrhosis
ACLF
hs VCAM-1
p<0.0002
p=0.0047
ns
ng/ml
Healthy
Cirrhosis
ACLF
C
Angiopoietin-2
Pathological control
Cirrhosis
ACLF
Ang-2
Ang-2
Ang-2
p=0.0317
p=0.0381
portal tracts
hepatic plates
% of Angiopoietin-2 signal
Control
Cirrhosis
ACLF

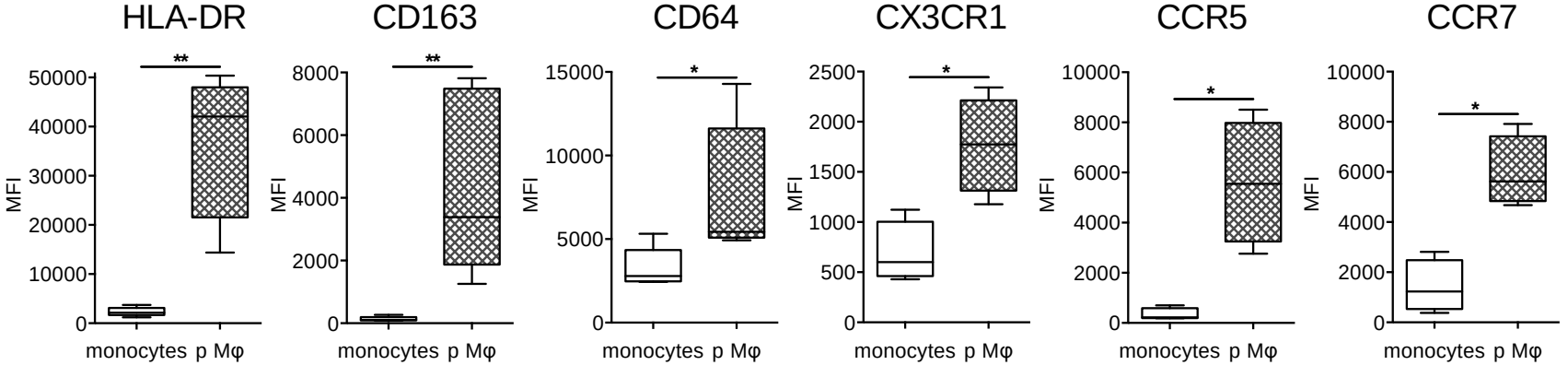
HLA-DR
CD163
CD64
CX3CR1
CCR5
CCR7
MFI
**
**
*
*
*
*
50000
40000
30000
20000
10000
0
8000
6000
4000
2000
15000
5000
2500
1500
1000
500
monocytes
p Mφ